Thesis for the Degree of Doctor of Philosophy

Outdoor heat in urban areas

Model development and applications

Nils Wallenberg

Department of Earth Sciences
Faculty of Science

UNIVERSITY OF GOTHENBURG

Gothenburg 2022

Outdoor heat in urban areas – Model development and applications

nils.wallenberg@gvc.gu.se

ISBN 978-91-8009-815-1 (PRINT)
ISBN 978-91-8009-816-8 (PDF)
ISSN 1400-3813
http://hdl.handle.net/2077/71430
A173

Printed in Borås, Sweden 2022
Printed by Stema Specialtryck AB

Till Klas

ABSTRACT

Heat waves and high outdoor air temperature can lead to heat stress with negative implications for human health and wellbeing such as heat stroke, heat cramps, dehydration and in extreme cases death. The urban population is at higher risk of such outcomes because of the generally warmer urban climate. Daytime outdoor thermal comfort is substantially affected by short- (solar) and longwave (thermal) radiation, i.e. mean radiant temperature (T_{mrt}). The overall aim in this thesis is to deepen the knowledge of radiant conditions in complex urban areas and how such knowledge can be utilized in modelling of T_{mrt} and thermal comfort of humans.

The overall aim is examined in three parts. The first part examines the effects of anisotropic (non-uniform) estimations of sky diffuse shortwave radiation and longwave radiation in the SOlar and LongWave Environmental Irradiance Geometry model (SOLWEIG) and how these influences T_{mrt} of humans in outdoor urban environments, compared to isotropic conditions. The results show that anisotropic sky diffuse shortwave radiation and longwave radiation are important in estimations of T_{mrt}. The circumsolar and horizon regions irradiates more diffuse shortwave radiation when the sky is anisotropic, which increases radiant load mainly in sunlit areas. Anisotropic sky longwave radiation increases with zenith angle, reaching its maximum at the horizon, resulting in higher T_{mrt} in open areas where the horizon region is visible.

The second part focuses on outdoor thermal comfort of preschoolers in Sweden in the present and future climate using SOLWEIG. It is concluded that two thirds of preschool yards in Gothenburg have 50% or more of their yard area exposed to strong heat stress. Heat stress in preschools lead to drowsy, tired and overheated children, with negative consequences for the pedagogical activities, forcing teachers to ensure that children stay cool on the expense of education. Heat stress days are expected to increase in the future, potentially exacerbating already existing heat related issues. However, with abundant tree shade heat stress is limited, both in the present and in the future.

In the third part optimized locations for trees to mitigate excessive T_{mrt} with regards to the shading effect of trees is analyzed. Tree positions depend on tree size and what time of day when shading is required.

The results of this thesis highlights the significance of realistic models, importance of applied studies to identify heat related problems and how such problems can be mitigated.

SAMMANFATTNING PÅ SVENSKA

Värmeböljor och höga utomhustemperaturer kan leda till värmestress med negativa följder på mänsklig hälsa och välmående, t.ex. värmeslag, kramper, uttorkning och i extrema fall död. Den urbana befolkningen är extra utsatt för värmestress på grund av det generellt sett varmare urbana klimatet. Dagtid är den termiska komforten utomhus i stora drag påverkad av kort- (sol) och långvågig (termisk) strålning, dvs strålningstemperatur (T_{mrt}). Det övergripande syftet med denna avhandling är att fördjupa förståelsen och kunskapen om strålningsförhållanden i urbana områden och hur sådan kunskap kan användas i modellering av T_{mrt} och termisk komfort hos människor.

Det övergripande syftet är utvärderat i tre delar. Den första delen fokuserar på anisotropa (olikformiga) modellberäkningar av diffus strålning från himlen och långvågig strålning i SOlar and LongWave Environmental Irradiance model (SOLWEIG) och hur dessa påverkar T_{mrt} i urbana utomhusmiljöer, jämfört med isotropa (likformiga) förhållanden. Resultaten visar att anisotropa strålningsförhållanden är viktiga i beräkningar av T_{mrt}. Med den anisotropa himlen ökar T_{mrt} i solbelysta områden på grund av den högre andelen diffus strålning från områden kring solen och längs horisonten. Anisotrop långvågig strålning från himlen ökar med zenitvinkel och når sitt maximum nära horisonten, vilket leder till ökad T_{mrt} i öppna områden där horisonten är synlig.

Den andra delen fokuserar på termisk komfort hos förskolebarn i svensk utomhusmiljö. Här visar resultaten att på två tredjedelar av alla förskolegårdar i Göteborg är 50% eller mer av ytan exponerad för hög värmestress. Värmestress på förskolor leder till dåsiga, trötta och överhettade barn, med negativa konsekvenser för den pedagogiska verksamheten, då lärarna måste se till att barnen håller sig svala på bekostnad av undervisningen. Dagar med värmestress förväntas öka i framtiden och förvärra redan existerande värmerelaterade problem. Om det däremot finns rikligt med skugga från träd är värmestressen begränsad, både nu och i framtiden.

I den tredje delen analyseras optimerad positionering av träd för att minska T_{mrt} med hjälp trädens skuggeffekt. Trädens positioner beror på trädens storlek och vilken tid på dagen som skuggeffekten är viktig.

Resultaten i denna avhandling visar på vikten av realistiska modeller, betydelsen i applicerade studier för att identifiera värmerelaterade problem och hur sådana problem kan minskas.

ACKNOWLEDGEMENT

I would like to thank all my friends and colleagues at the Department of Earth Sciences, University of Gothenburg, who turned my PhD studies into five years of fun. A sincere thank you to my supervisors for giving me the opportunity to do this and for all the supervision and support throughout. Thank you Fredrik Lindberg for patiently listening to all my questions, always supporting me and getting me into Python and QGIS. Thank you Sofia Thorsson for always listening and your helpful comments to improve my texts. Thank you David Rayner for being an infinite source of fantastic ideas. A special thank you to Björn Holmer for support and contributing with your immense knowledge on urban climate. Thank you Deliang Chen, my examiner, for valuable advice.

Thank you Oskar for much appreciated discussions and Janka for fun times in Australia (we have to finish the paper). Thank you my dearest fika friends, Michelle and Julia. Thank you Zach for great office chats. Thank you Oskar, Julia and Cole for being opponents in my half-time and final seminars. Thank you all current and former PhD students and thank you all lunch and fika friends for great discussions about everything and nothing.

I also want to thank my family for always supporting me and giving encouraging words, tack mamma, pappa, Simon, Daniel, Fredrik, farmor, farfar, Linda, Haben, Aris, Nemi, Nico, fastrar, morbror, kusiner. A special thank you to Cicci, my love. Thank you Lovisa, great friend and number one fan of my PhD studies. Thank you Viktor, Johan, Jenny, Karin, Andreas, Gunnar and many more.

Thank you all my friends outside of academia for concerts, discussions, laughs, walks, travels and letting me know that there is more to life than work.

LIST OF ARTICLES

This thesis is based on the following articles, referred to in the text by their Roman numerals:

I. **Wallenberg, N.**, Lindberg, F., Holmer, B. and Thorsson, S. 2020. The influence of anisotropic diffuse shortwave radiation on mean radiant temperature in outdoor urban environments. *Urban Climate*. 100589. https://doi.org/10.1016/j.uclim.2020.100589

NW led the model development and prepared the original draft. FL, BH and ST provided overall supervision as well as review and editing of the original draft.

II. **Wallenberg, N.**, Holmer, B., Lindberg, F. and Rayner, D. n.a. An anisotropic parameterization scheme for longwave irradiance and its impact on radiant load in urban outdoor settings. *Submitted to International Journal of Biometeorology*.

NW led the model development and prepared the original draft. BH, FL and DR provided overall supervision as well as review and editing of the original draft.

III. Bäcklin, O., Lindberg, F., Thorsson, S., Rayner, D. and **Wallenberg, N**. 2021. Outdoor heat stress at preschools during an extreme summer in Gothenburg, Sweden – Preschool teacher's experiences contextualized by radiation modelling. *Sustainable Cities and Society*. 75: 103324. https://doi.org/10.1016/j.scs.2021.103324

OB prepared model simulations, conducted interviews and wrote the original draft. FL and **NW** supported in preparing model simulations. All authors reviewed and edited the original draft.

IV. **Wallenberg, N.**, Rayner, D., Lindberg, F. and Thorsson, S. n.a. Present and future thermal (dis)comfort of preschoolers in five Swedish cities. *Manuscript.*

NW ran the model simulations and prepared the original draft. **NW** and DR prepared the input data. FL and ST provided overall supervision as well as review and editing of the original draft.

V. **Wallenberg, N.**, Lindberg, F. and Rayner, D. 2022. Locating trees to mitigate pedestrian heat stress in urban areas using a metaheuristic hill-climbing algorithm. *Geoscientific Model Development*. 15: 1107-1128. https://doi.org/10.5194/gmd-15-1107-2022

NW led the model development and prepared the original draft. FL and DR provided overall supervision as well as review and editing of the original draft.

CONTENT

1 INTRODUCTION

The urban population is projected to reach 68 % of the world's total population by 2050, compared to approximately 55 % in 2018 (UN, 2018). In Sweden approximately 9.1 million, or 88% of the population, live in urban areas (SCB, 2022a).

The summer of 2018 was one of the hottest in Sweden since recordings began (Wilcke et al., 2020). Clear, warm and dry weather led to drought with forest fires (Krikken et al., 2021), decreases in harvests and increased tree mortality (Buras et al., 2020) as destructive consequences with large impacts on society. Air temperature (T_{air}) (Christensen et al., 2022) and number of heat waves similar to the one in 2018 are projected to increase in Sweden in the future (Nikulin et al., 2011). Hot weather and heat waves can have large negative impacts on human health and wellbeing e.g. heat stroke, dehydration, heat exhaustion and heat cramps and in extreme cases death (Kovats & Hajat, 2008). Åström et al. (2019) attributed an excess 601-750 deaths to the long-lasting hot weather of 2018. According to Oudin Åström et al. (2013) climate change is accountable for a doubling in heat related mortality in Sweden 1980-2009. The urban population is at higher risk of morbidity and mortality from heat waves (Gabriel & Endlicher, 2011), due to the relatively warm urban climate. During clear nights with low wind speed (WS) the local urban climate is characterized by higher T_{air} compared to its surrounding rural areas (Ackerman, 1985; Eliasson, 1996), a phenomenon referred to as urban heat island (UHI) (Oke, 1982). In periods with hot daytime weather and potential heat stress, cool nighttime T_{air} is important for recovery (Rocklöv et al., 2011).

Daytime heat stress of humans is influenced to a large extent by radiant load, i.e. how much solar (hereafter referred to as shortwave) and thermal (hereafter referred to as longwave) radiation that a human is exposed to (Mayer & Höppe, 1987; Thorsson et al., 2007; Lindberg et al., 2016). Radiant load, compared with T_{air}, have large spatial variations depending on if a person is exposed to shortwave radiation and if surrounding surfaces are shaded or sunlit (Lindberg et al., 2016).

Awareness of harmful levels of heat is ever increasing even in a country like Sweden that in the eye of the public is often considered a cold location. The

Public Health Agency of Sweden recently released a report on heat stress in urban outdoor environments (Folkhälsomyndigheten, 2018), focusing on identification, mitigation and adaptation, for use by e.g. stakeholders and planners. In 2018 the Swedish government appointed the National Expert Council on Climate Adaptation with the objective to compile and evaluate the process and work of Swedish municipalities, regions, country administrative boards, public authorities and private actors in climate adaptation (Klimatanpassningsrådet, 2022). In February 2022 they released their first report with the intention to serve as a basis for the Swedish government in the continuation and future work on climate adaptation. The importance of knowledge on built-up areas and its relation to human health is dedicated in an explicit chapter in the report, demonstrating the importance of this subject.

Increasing urban greenery is a common alternative in mitigation of outdoor heat in urban areas (e.g. Klimatanpassningrådet, 2022; Konarska et al., 2014). The 11th target of The United Nations (UN) Sustainability Development Goals (SDG) is

> "Make cities and human settlements inclusive, safe, resilient and sustainable" (UN, 2015)

where objective 11.7 is to

> "By 2030, provide universal access to safe, inclusive, and accessible, green and public spaces, in particular for women and children, older persons and persons with disabilities."

In addition, objective 11.b is

> "By 2020, substantially increase the number of cities and human settlements adopting and implementing integrated policies and plans towards inclusion, resource efficiency, mitigation and adaptation to climate change, resilience to disasters, and develop and implement, in line with the Sendai Framework for Disaster Risk Reduction 2015-2030, holistic disaster risk management at all levels"

SDG 11.7 and 11.b are closely associated with SDG 3:

> "Ensure healthy lives and promote well-being for all at all ages" (UN, 2015)

indicating the importance of vegetation to mitigate and regulate heat in urban areas.

Given the immense amount of people residing in urban areas, the expected increase in urban population, combined with the generally warmer urban climate and a projected warmer future climate demands for an increase in knowledge of the urban climate, its relation to human health and wellbeing and mitigation of hazardous heat.

1.1 URBAN CLIMATE

Urban climate has been studied for around 200 years (Howard, 1833) and has a relatively long history in Sweden as well with studies reaching back some 70 years, investigating the urban climate in Uppsala (Sundborg, 1950; 1951). The built-up characteristics of urban areas, i.e. buildings, materials, street orientation, lack of permeable surfaces and lack of vegetation influences the urban climate. The general outcome of this is a higher T_{air} compared to the surrounding rural areas, particularly in nighttime, i.e. UHI (Oke, 1982). Street geometries are important for exposure to and release of energy. Nighttime cooling rate is slow in dense street canyons and faster in open areas (Holmer et al., 2007). Street orientation influences exposure to shortwave radiation, where north-south oriented streets would be sunlit mainly midday when the sun is in the south (northern hemisphere) (Erell & Williamson, 2007; Erell et al., 2014). Urban areas predominantly consist of impervious materials e.g. concrete, brick, stone and asphalt (Oke, 1982). These materials have high thermal admittance, absorbing energy during the day, which increases their surface temperatures, i.e. sensible heat flux (Oke, 1981). The high thermal admittance lead to slow emittance of energy at night with a resulting slow cooling rate (Oke, 1981). This can be compared to wood that have comparably low thermal admittance, meaning that it absorbs and releases energy rapidly. Thus, cooling rates in urban areas are relatively slow compared to rural areas. Colors of building materials influences absorption, with brighter colors normally reflecting more than darker colors (Fallman et al., 2013; Erell et al.,

2014). The typically lower albedo of urban areas compared to rural areas (Oke, 1988) leads to an increased absorption of shortwave radiation, resulting in higher sensible heat flux. The overall lack of permeable surfaces and vegetation, likewise, increases sensible heat flux as less energy goes into latent heat flux (Oke, 2017). Vegetation, for example, transpires, increasing latent heat on the expense of sensible heat (Oke, 1982; Holmer et al., 2013). There is also an influence from anthropogenic heat, e.g. combustion of fuels and heating of buildings (Oke, 1988). Moreover, UHI increases with size of the city (Oke, 1973; Zhou et al., 2017).

Even though the description above refers to UHI the determining factors can have direct negative effects on daytime outdoor human thermal comfort.

1.2 DAYTIME OUTDOOR HUMAN THERMAL COMFORT

Thermal comfort refers to when an individual feel or show no signs of heat stress and the human energy balance is close to a net zero with no gain or loss of heat (Oke et al., 2017). Daytime outdoor human thermal comfort is largely influenced by four meteorological variables: T_{air}, humidity, WS and radiant load. While all four variables are important for outdoor human thermal comfort, the main focus of this thesis is radiant load. One way of estimating radiant load on a human is with mean radiant temperature (T_{mrt} [°C]). T_{mrt} essentially describes the exchange of shortwave and longwave irradiance between a human and its surroundings, i.e. the radiant heat load (Höppe, 1992; Thorsson et al., 2007). T_{mrt} is defined by the American Society of Heating, Refrigerating and Air Conditioning Engineers (ASHRAE, 2001) as "the uniform temperature of an imaginary enclosure in which radiant heat transfer from the human body equals the radiant heat transfer in the actual non-uniform enclosure".

1.2.1 MEAN RADIANT TEMPERATURE (T_{MRT})

T_{mrt} is an important meteorological variable in indices for outdoor human thermal comfort (Mayer et al., 2008), e.g. COMfort FormulA (COMFA) model (Brown & Gillespie, 1986), the Physiological Equivalent Temperature (PET [°C]) (Mayer & Höppe, 1987; Höppe, 1999; Matzarakis et al., 1999) and the Universal Thermal Climate Index (UTCI [°C]) (Blazejczyk et al., 2010).

On hot days largest fraction of T_{mrt} on a human in outdoor urban environments is attributed to longwave radiation from surrounding warm surfaces such as vegetation, buildings and the atmosphere (Lindberg et al., 2014). Shortwave radiation originates from the sun (Thorsson et al., 2007; Lindberg et al., 2008) and is composed of a direct component originating directly from the sun, a diffuse part scattered on particles in the atmosphere and one part reflected on surfaces, e.g. buildings and vegetation (Lindberg et al., 2008). Exposure to shortwave radiation, thus, depends to large part on whether an area is sunlit or in shade. Longwave radiation is largely influenced by the emissivity and temperature of the emitting source. Down-welling sky longwave radiation correlates with the emissivity of the sky and T_{air} (Prata, 1996; Jonsson et al., 2006). The amount of longwave radiation emitted by a surface, likewise, depends on its emissivity and surface temperature (Lindberg et al., 2016). A sunlit surface would, for example, have a higher surface temperature and thus emit more longwave radiation than if it was in shade (Lindberg et al., 2016; Vanos et al., 2016). Emissivity is basically the potential of a material to emit longwave radiation and amount of emitted longwave radiation is largely dependent on the temperature of the material.

The effects of built-up areas on short- and longwave radiation varies, but are to some extent similar to those affecting the UHI. A white-painted wall in general have a high albedo and would normally reflect a large part of the incoming shortwave radiation, resulting in a decrease in surface temperature of the wall and thus diminished longwave emittance (Erell et al., 2014). For pedestrians, on the other hand, this would lead to an increase in exposure to shortwave radiation (Erell et al., 2014), resulting in an increased T_{mrt}. Vegetation generally emits low amounts of longwave radiation, especially compared to a sunlit building surface (Lindberg et al., 2016). Similarly, a tree can block the direct shortwave component from the sun (Konarska et al., 2014), casting shadows on ground surfaces and building facades, decreasing their longwave emittance (Vanos et al., 2016). The H/W ratio, likewise, influences exposure to shortwave radiation in street canyons, where high H/W in general blocks the direct component (Erell & Williamson, 2007; Erell et al., 2014). This, however, depends on the street orientation. Accordingly, T_{mrt} can vary substantially in urban areas, with highest values normally found in front of sunlit walls and lowest in areas shaded by e.g. trees or buildings (Lindberg et al., 2014; Thorsson et al., 2017). An increase in amount of absorbed radiation

increases the radiant load on a human and impairs thermal comfort (Mayer et al., 2008).

1.2.2 THERMAL COMFORT AND THE HUMAN ENERGY BALANCE

There are two factors to consider when studying outdoor thermal comfort of humans: meteorology and human energy balance (where meteorology plays a large part) (Brown & Gillespie, 1986; Höppe, 1999; Blazejczyk et al., 2010).

The meteorological variables that have considerable impact on thermal comfort of humans and the human energy balance are T_{air}, T_{mrt} (section 1.2.1), humidity and WS. Humidity influences sweat rate of humans (Kenny et al., 2009a; 2009b). Wind can also have a cooling effect on a human during hot weather conditions as it would remove heat from the body and increase convective heat loss (Vanos et al., 2012b).

Following is one example of how the human energy balance (B) can be described (Brown & Gillespie, 1986; Kenny et al., 2009a):

$$B = M + R_{abs} - C - E - L \quad (1)$$

where M is the metabolic heat production, R_{abs} is absorbed radiation (short- and longwave described in 1.2.1), C is convective heat loss, E is evaporative heat loss and L is emitted longwave radiation.

Some of the metabolic heat is lost through respiration and sensible heat flux (Brown & Gillespie, 1986). The remaining heat is transferred from the core of the body to the surface, i.e. skin where it is lost to convection (C), evaporation (E) and emitted as longwave radiation (L). M is influenced by metabolic rate, which is influenced by the activity at hand. A more physically demanding activity results in higher M (Butte et al., 2018). Moreover, M is influenced by age, gender, weight and length, where a child would have slightly lower metabolic rate (kJ h^{-1}) compared to an adult (Schofield, 1985), but higher body-surface-area to body-mass ratio (BSA:BM), which influences the M (Cheng & Brown, 2020). Furthermore, a boy have higher M compared to a girl (Schofield, 1985).

Convective heat loss (C) is essentially the sensible heat loss from the core of the body, conducted through the skin, clothing and eventually the boundary layer of the person (Brown & Gillespie, 1986; Höppe, 1999; Kenny et al., 2009).

Some heat is lost through evaporative heat loss (E) or perspiration (Brown & Gillespie, 1986; Höppe, 1999; Kenny et al., 2009).

A part of the heat produced or absorbed by the body is emitted as longwave radiation (L) from the skin or clothing (Brown & Gillespie, 1986).

There are many thermal comfort indices, incorporating the human energy balance, available when investigating perceived weather by humans in outdoor environments. Three examples are given in the following subsections: COMFA (1.2.3), PET (1.2.4) and UTCI (1.2.5).

1.2.3 COMFORT FORMULA (COMFA)

The COMFA model is a predictor of thermal sensation at different levels of activity, e.g. walking and running (Brown & Gillespie, 1986; Kenny et al., 2009a; 2009b; Vanos et al., 2012a; 2012b; 2012c; 2017; Cheng & Brown, 2020; Liu & Jim, 2021).

The COMFA model is initially based on the work by Fanger (1970), with recent developments by Kenny et al. (2009a; 2009b), Vanos et al. (2012a; 2012b; 2012c) and Cheng and Brown (2020). Cheng and Brown (2020) altered three of the physiological characteristics that differs between a child and an adult, metabolic heat production, sweat rate and BSA:BM, to make the model more fit for a child (referred to as COMFA-kid). While PET (1.2.4) and UTCI (1.2.5), for example, gives an output in °C, COMFA has a slightly more abstract way of describing it in Wm^{-2}. The output Wm^{-2} is compared to a scale that determines the thermal sensation. Nevertheless, COMFA is a dynamical model, sensitive to physical activity, clothing and physiological characteristics such as age, height and weight. In comparison, PET and UTCI are developed for adults, even though it is possible to change the physiological characteristics in PET to fit that of a child (but with little difference in the end result). COMFA and COMFA-kid, on the other hand, are more sensitive to physiological changes.

Required meteorological input to COMFA are down-welling and outgoing short- and longwave radiation, T_{air}, relative humidity (RH) and WS. Furthermore, information on metabolic heat production, clothing, gender, age, length and weight are necessary.

1.2.4 PHYSIOLOGICAL EQUIVALENT TEMPERATURE (PET)

PET is a common thermal comfort index in evaluations of perceived weather conditions by humans (Mayer et al., 2008; Matzarakis et al., 1999; Lee et al., 2013). PET (Mayer & Höppe, 1987; Höppe, 1999; Matzarakis et al., 1999) is based on the Munich Energy balance Model for Individuals (MEMI) (Höppe, 1984; 1994) and in short describes how outdoor weather conditions would be experienced by translating them to indoor conditions. For example, in a room where T_{air} = 21 °C, $T_{mrt} = T_{air}$, WS = 0.1 ms^{-1} and RH = 50% the estimated PET = 21 °C (Höppe, 1999). In this sense it is relatively easy to interpret what it would feel like if PET = 30 °C by imagining a room with T_{air} = 30 °C.

Required meteorological variables to calculate PET are T_{air}, T_{mrt}, RH and WS. Physiological input requirements are gender, age, weight, length, metabolic heat production and clothing.

1.2.5 UNIVERSAL THERMAL CLIMATE INDEX (UTCI)

UTCI (Blazejczyk et al., 2010) is based on the Fiala model (Fiala et al., 2012). The advantage with UTCI compared to many other thermal comfort indices is that it only requires T_{air}, RH, T_{mrt} and WS as inputs. The disadvantage, on the other hand, is that the physiological characteristics governing the human energy balance are embedded in its linear relationship. UTCI is always estimated for a 73.5 kg, 14% body fat content and 1.86 m^2 Dubois-area person. Moreover, clothing changes with T_{air}, where this average person would wear less clothing in hotter weather and vice versa.

1.3 ESTIMATING OUTDOOR HUMAN THERMAL COMFORT IN URBAN ENVIRONMENTS

1.3.1 FIELD MEASUREMENTS OF T_{MRT}

There are different ways of estimating T_{mrt} from field measurements, e.g. radiation measurements (Höppe, 1992) or with a globe thermometer (Nikolopoulou et al., 1999). The most detailed and complex methods as of now is the one developed by Höppe (1992). Höppes method, also known as the 3D integral radiation measurements, includes three net radiometers that measures the incoming shortwave (with a pyranometer) and longwave (with a pyrgeometer) radiation from all cardinal directions (north, south, east and west) as well as from above and below. This is the most common method in field measurements for estimation of T_{mrt}. Nevertheless, anomalies has been described in studies by e.g. Thorsson et al. (2007) and Kántor et al. (2014). The anomalies are depicted by a local minimum around noon, as well as a slight overestimation just prior to and after noon, which all relate to the shape of the standing human in this method, which is represented by a standing box. Some of these anomalies have been corrected for by e.g. Holmer et al. (2015), where a human is instead represented by a cylinder.

1.3.2 SIMULATING RADIANT LOAD AND THERMAL COMFORT

Field measurements with e.g. Höppes (1992) method (see section 1.3.1) give accurate estimations of T_{mrt}. On the other hand, field measurements only depict the conditions for a single location, i.e. where the equipment is located. Another approach, making it possible to cover larger areas, is through modelling. There are a number of radiation models for micro-climate commonly used within the field of urban climate, e.g. ENVI-Met (Bruse & Fleer, 1998; Simon, 2016), RayMan (Matzarakis et al., 2007; 2010), SOLWEIG (Lindberg et al., 2008), SOLENE-microclimate (Musy, et al., 2015) and PALM4U (Maronga et al., 2015). Such models are important for urban planning and design and can work as a bridge between climatologists and e.g. landscape architects (Brown, 2011). A general shortcoming with models is that they need to parameterize certain processes, i.e. simplify, different natural processes or make assumptions that are not always true. As

an example, the sky can be considered as isotropic for diffuse shortwave irradiance. Assuming an isotropic sky for diffuse shortwave irradiance means that diffuse shortwave irradiance is equal from all parts of the sky. Nevertheless, observations by e.g. Perez et al. (1993) have shown that this is not the case, and that sky diffuse shortwave irradiance in fact is relatively high in the circumsolar region and along the horizon, compared to other parts of the sky on clear days. Robinson & Stone (2004; 2005) clarified the results by Perez et al. (1993) by developing a model based on the work by the latter, where the sky is divided into 145 patches. Their results signified the importance of using an anisotropic model for diffuse shortwave irradiance in building energy models in urban areas where obstacles such as buildings can block parts of the sky, e.g. the circumsolar region or the horizon. In studies on human thermal comfort, on the other hand, omitting anisotropic diffuse shortwave radiation could have impacts on simulated radiant load and heat stress.

1.4 WARM WEATHER AND HUMAN HEALTH

The importance of accurate tools and models for estimation of heat stress and identification of e.g. temperature thresholds or exposed areas are associated with human health and its relation to hot weather.

1.4.1 HEALTH IMPACTS

It is important to identify areas where humans are at risk of excessive heat during hot weather conditions that can lead to e.g. heat stroke, dehydration and heat exhaustion (Kovats & Hajat, 2008). Rocklöv and Forsberg (2008) found an optimal mean daily T_{air} for Stockholm, Sweden of 11-12 °C. Outside this range the risk of morbidity and mortality increased and the risk of warm weather was larger compared to cold weather. Evaluations of thermal comfort and heat stress of humans in outdoor urban environments can be achieved by studying T_{mrt} and different indices e.g. COMFA, PET and UTCI. While T_{mrt} should be used with caution, as it only describes the radiant load of a human, it is a good predictor and indicator of heat stress. Thorsson et al. (2014) found that high daytime T_{mrt} correlated with heat related mortality among people aged 80+, whereas high nighttime T_{mrt} correlated with heat related mortality among peopled aged 45-79. Thermal comfort indices like COMFA (Brown & Gillespie, 1986), PET (Höppe, 1999; Matzarakis et al., 1999) and UTCI (Blazejczyk et al., 2010) have scales corresponding to several levels of

perceived thermal sensation e.g. moderate heat stress or when hot weather potentially is harmful or even dangerous.

Groups that are at higher risk of morbidity and mortality from warm weather are children, elderly, chronically ill (with respiratory and/or cardiovascular diseases), pregnant, people with physical and/or mental disabilities and people consuming certain medication (Folkhälsomyndigheten, 2015; 2017).

1.4.2 WARM WEATHER AND CHILDREN

Children are identified as a vulnerable group because of their limited experience of heat, reflected in their inability to react to thermal discomfort (Vanos et al., 2017; Cheng & Brown, 2020) and differing physiological characteristics, e.g. reduced sweat rate (Falk & Dotan, 2008; Shannon et al., 2009), BSA:BM (Vanos et al., 2017; Cheng, 2020) and higher heat production (Falk & Dotan, 2008). Their limited or missing experience of heat increases their risk of being affected by heat related problems e.g. dehydration, heat stroke, heat exhaustion (Kovats & Hajat, 2008), as they may not understand the potential danger or effect of heat on their health (Vanos et al., 2017; Cheng & Brown, 2020).

A larger BSA:BM influences exposure to and absorption of short- and longwave radiation (Cheng, 2020). In addition to this, children's core temperature rises faster than that of an adult (Falk & Dotan, 2008). Furthermore, the core of their body is closer to a potentially hot ground surface (Vanos et al., 2017).

The reduced sweat rate of children influences their ability to cool during hot weather (Falk & Dotan, 2008). Under normal conditions, thermoregulation of children is comparable to adults. In hot weather, on the other hand, when skin temperature is lower than T_{air} their BSA:BM increases the absorption of heat, while their reduced ability to sweat is insufficient to cool (Falk & Dotan, 2008).

Moreover, Swedish preschoolers spend about three hours per day outdoors (Mårtensson, 2004). There are general recommendations that young children, age 0-5, have the possibility move around and outdoor activities are endorsed (Folkhälsomyndigheten, 2021). For older children, age 6-17, 60 minutes of moderate physical activity per day is recommended.

1.5 MITIGATING EXCESSIVE RADIANT LOAD

As previously mentioned, T_{mrt} or radiant heat load is important in governing the human energy balance and outdoor thermal comfort (Mayer et al., 2008). Excessive radiant load can have a negative effect on human health (Thorsson et al., 2014), manifesting the importance of mitigating measures. Highest radiant heat load occurs on clear and warm days when the clear sky allows for high intensity of shortwave radiation to reach pedestrians and surfaces at street level and the warm weather contributes to relatively high emittance of longwave irradiance (Thorsson et al., 2007). On such days areas in front of sunlit walls are exposed to high radiant load (Thorsson et al., 2017) with highest fraction of irradiance being associated with longwave radiation (Lindberg et al., 2014). However, longwave radiation is difficult to regulate. The shortwave component originating from the sun is, on the other hand, easier to manipulate by blocking the direct component with e.g. a tree or a building, i.e. shading (Lindberg & Grimmond, 2011). Shading by buildings is an option, but increasing the fraction of buildings in already built-up areas as well as altering already existing buildings can be difficult. Another shade-providing option is trees (Konarska et al., 2014; Lindberg et al., 2016), which are relatively easy to implement. There are many studies on the topic of vegetation as a mitigating tool for excessive radiant load, e.g. Zhao et al. (2018), Abdi et al. (2020), Lee et al. (2020) and Srivanit and Jareemit (2020). However, such studies rarely look at the optimal position of trees for mitigation of excessive radiant load. There are some studies focusing on optimization of tree positioning for e.g. lowering energy demand in buildings with an increase in tree shade (Zhao et al., 2017). A few studies have however studied optimization of tree locations for mitigation of radiant load by utilizing metaheuristic algorithms (Chen et al., 2008; Ooka et al., 2008; Zhao et al., 2017; Stojakovic et al., 2020). Metaheuristic algorithms can help find acceptable solutions to problems where the answer is unknown and brute-force calculations would be too extensive and thus not feasible (Luke, 2013). Nevertheless, studies on optimal positioning of trees to mitigate radiant load and increase thermal comfort are scarce, but important for urban planning and design.

2 AIM

A projected warmer future climate in parallel to an expected growing urban population that includes groups vulnerable to heat gives high incentive for bringing the field of urban climatology forward. The overall aim in this thesis is to deepen the knowledge of radiation conditions in complex urban areas and how such knowledge can be utilized in modelling of outdoor radiant load and thermal comfort of humans.

The specific aims in this thesis are to:

i. Assess the importance of anisotropic sky diffuse shortwave radiation (**Paper I**) and anisotropic longwave radiation (**Paper II**) on radiant load of humans in outdoor urban environments, utilizing empirically derived anisotropic models.
ii. With microclimate modeling, evaluate radiant load on preschool yards in Gothenburg, Sweden, and the potential impact on preschoolers in the present climate (**Paper III**) and potential consequences of future climate change on thermal comfort of preschoolers in Sweden (**Paper IV**).
iii. Exploit metaheuristic algorithms to examine optimized tree positioning for heat mitigating measures in urban areas (**Paper V**).

3 DATA AND METHODS

3.1 STUDY AREAS

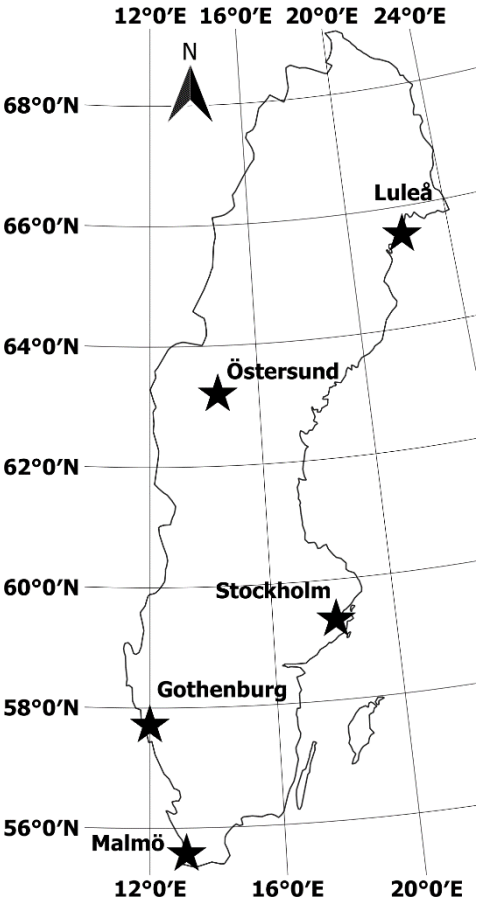

Figure 1. Map of Sweden with locations (stars) used in this thesis.

The main part of the simulations (**Papers I-V**) and field measurements (**Paper II**) in this thesis are conducted in Gothenburg, Sweden. Gothenburg is the second largest city in Sweden with ~587 000 inhabitants (SCB, 2022b). The climate is cold with mild to cold winters although summers are relatively warm for Swedish standards (Köppen-Geiger classification Dfb) (Beck et al., 2018) and is influenced by the westerlies with alternating low- and high pressure systems (Thorsson et al., 2011). In **Paper IV** four additional Swedish locations are used: Malmö, Stockholm, Östersund and Luleå. Malmö is the third largest city in Sweden with a population ~352 000 (SCB, 2022b). The climate is similar to that of Gothenburg. Sweden's largest city and capital is Stockholm with ~979 000 inhabitants and is likewise classified as Dfb in the Köppen-Geiger climate classification system (Beck et al., 2018). Östersund is located in the Scandinavian mountains, with a more continental climate. The population is ~64 000 and it is located at ~300 masl. Luleå, with ~79 000 inhabitants, is the most northern city studied in this thesis. Luleå and Östersund have cold climates with cold winters and relatively cold summers (Dfc). All locations except Östersund are located by the sea, i.e. on average only a few meters above sea level, and are therefore influenced by the sea. The locations are depicted in fig. 1.

3.2 OUTDOOR THERMAL COMFORT OF HUMANS

3.2.1 SOLWEIG

The SOlar and LongWave Environmental Irradiance Geometry (SOLWEIG) model is a 2.5D model solving 3D short- and longwave radiation fluxes and T_{mrt} (Lindberg et al., 2008) in complex urban settings. It is a fast model that requires few input data. Required input to SOLWEIG are a raster (grid) Digital Surface Model (DSM) with building and ground elevation, meteorological data (T_{air}, RH and global shortwave radiation (G) or incoming direct and diffuse shortwave irradiance) for given time steps. Additional optional inputs are a canopy DSM (CDSM) for tall vegetation (e.g. trees) (Lindberg & Grimmond, 2011) and data on ground cover (to differentiate emissivity and albedo of various surfaces, e.g. grass and asphalt) (Lindberg et al., 2016). Moreover, if meteorological data on WS is available it is possible to estimate PET and UTCI. In SOLWEIG a standing person is represented by a vertical cylinder (Holmer et al., 2015). SOLWEIG is used in all papers in this thesis.

Paper IV utilizes a 1D version of SOLWEIG. In this 1D version of SOLWEIG radiation fluxes and T_{mrt} are estimated for a single location. Using the new parameterization schemes described in **Papers I** and **II** it is possible to generate locations where the upper hemisphere, made up of 153 parts (see section 3.2.4), is divided into different surfaces. These can be thought of as coarse resolution sky view images, i.e. a sky view image made up of 153 pixels. This 1D version of SOLWEIG is utilized in **Paper V** as well although without the parameterization schemes presented in **Papers I** and **II**.

3.2.2 INPUT RASTER DATA IN SOLWEIG

Information on tall vegetation (CDSM) is used in **Papers II, III** and **V** and information on ground cover is used in **Papers II** and **III**. In **Paper III** DSM, CDSM and ground cover grid data for 440 preschool yards in Gothenburg are used. The preschools have a 100 m buffer zone surrounding the yards to include shading and radiation from surrounding objects. The spatial resolution of all raster data utilized in this thesis is 1 m, estimated from LiDAR measurements. The raster data were retrieved from the City Planning Authority of Gothenburg.

3.2.3 INPUT METEOROLOGICAL DATA IN SOLWEIG

Input meteorological data (T_{air}, RH, incoming shortwave radiation and WS (**Paper IV**)) in **Papers I, III, IV** and **V** are from the Swedish Meteorological and Hydrological Institute (SMHI). In addition, in **Paper IV**, meteorological observations for Gothenburg from Rayner et al. (2021) are used. In **Paper II** meteorological input data into SOLWEIG are from a weather station at the roof of the Department of Earth Sciences, University of Gothenburg. In **Paper IV** G is used and differentiated into a direct and diffuse component following the methods by Reindl et al. (1990). **Papers I**, **II**, **III** and **V** have direct and diffuse shortwave radiation input data.

3.2.4 PARAMETERIZATION OF SHORT- AND LONGWAVE RADIATION IN SOLWEIG

Previous versions of SOLWEIG, prior to the ones presented in **Papers I** and **II**, estimated sky diffuse shortwave radiation and longwave radiation reaching a grid point in the raster data based on sky view factor (SVF) (Lindberg et al., 2008). The SVF ranges from 0 to 1 and can be described as the ratio of sky visible from a point, in this case a pixel in a DSM and/or CDSM. Not only did these parameterization schemes assume the sky-vault as isotropic for both sky diffuse shortwave and sky longwave radiation. They also made it difficult to give detailed information on directionality of radiation. Nevertheless, they gave a good approximation of the average radiation reaching a human in most locations. Furthermore, parameterization based on SVF is a fast and simple approach. On the other hand it has been shown in various studies that sky diffuse shortwave radiation is in fact anisotropic (McArthur & Hay, 1981; Perez et al., 1993), with a higher proportion of the radiation originating from close to the sun (referred to as circumsolar brightening) and along the horizon (referred to as horizon brightening). Moreover, sky longwave radiation increases with zenith angle, reaching its maximum along the horizon (Bliss, 1961; Unsworth & Monteith 1975; Martin & Berdahl, 1984). The parameterization schemes described in **Papers I** and **II** divides the sky-vault into a number of patches. In **Paper I** number of patches was determined to 145 (figure 2) and updated to 153 in **Paper II**.

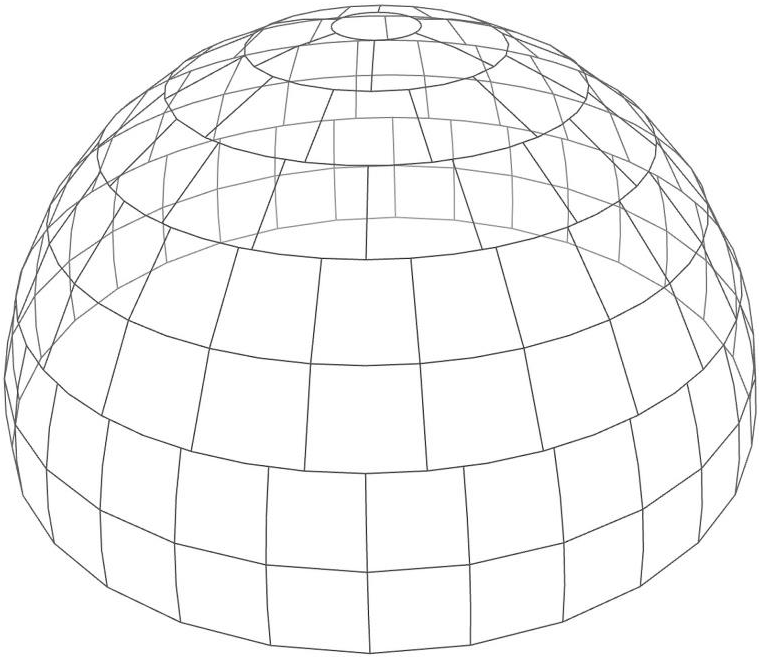

Figure 2. The sky vault divided into 145 patches according to Robinson and Stone (2004). Following **Paper II** the sky vault, in a similar way to this one, is divided into 153 patches (figure 1 in **Paper I**).

The parameterization scheme in **Paper I** is based on the methods by Robinson and Stone (2004; 2005). Their model, a sky radiosity algorithm (SRA), builds on previous work by Perez et al. (1993). The empirical model by Perez et al. (1993) estimates sky diffuse shortwave radiation for a given point on the sky-vault in relation to the position of the sun. The SRA divides of the sky-vault into 145 patches according by Tregenza (1987). Then the centroid of each patch represents the position in relation to the sun and amount of sky diffuse radiation can be determined from the solid angle of the patch.

In **Paper II** a parameterization scheme similar to the one in **Paper I** is used. Here, all longwave fluxes originating from the upper hemisphere are incorporated into the patches. A model for anisotropic sky longwave radiation is implemented where emissivity increases with zenith angle reaching its maximum along the horizon. Moreover, 153 patches as compared to 145 in **Paper I** are utilized. The knowledge on anisotropic sky longwave radiation has been around for almost 100 years (Dines & Dines, 1927; Elasser, 1942; Robinson, 1947; 1950; Awanou, 1998). The model by Martin and Berdahl

(1984) is used based on an evaluation by Nahon et al. (2019) of the models by Bliss (1961) and Martin and Berdahl (1984). The model by Martin and Berdahl (1984) showed good agreement with observations conducted by Nahon et al. (2019). A model by Unsworth and Monteith (1975) was also considered by the authors of **Paper II**, showing similar results as that of the model by Martin and Berdahl (1984). This model, on the other hand, under certain meteorological conditions, had emissivity exceeding 1, and was therefore excluded. Moreover, the shadow casting algorithm in SOLWEIG can differentiate between sky, buildings and vegetation. Thus, the shadow casting algorithm enables an additional implementation of building and vegetation surfaces in the parameterization scheme for longwave radiation. The estimation of longwave radiation originating from building and vegetation surfaces still uses the equations in previous versions of SOLWEIG, but estimated based on solid angle of the patch instead of SVF. This has facilitated determination of direction of longwave radiation. Here, as compared to the parameterization scheme for sky diffuse shortwave radiation, number of patches is set to 153 to decrease the difference in solid angle between patches. Accordingly, 153 patches are used in the parameterization for sky diffuse shortwave radiation following **Paper II**.

3.2.5 MEAN RADIANT TEMPERATURE (T_{MRT})

T_{mrt} is estimated from short- and longwave radiation fluxes and is used in all papers in this thesis. The short- and longwave radiation fluxes and the corresponding T_{mrt} is estimated using SOLWEIG (described in sections 3.2.1 – 3.2.4).

In previous versions of SOLWEIG T_{mrt} was estimated from short- and longwave radiation emanating from north, south, east, west, above and below (Lindberg et al., 2008). The developments of two new parameterization schemes in **Papers I** and **II** have enabled estimations of T_{mrt} from anisotropic sky diffuse shortwave (**Paper I**) and anisotropic longwave (**Paper II**) radiation. Short- and longwave radiation reflected on or emitted from ground surfaces are still estimated from the cardinal directions. The T_{mrt} estimated in SOLWEIG is used as input when calculating PET (sections 1.2.4 and 3.2.6) and UTCI (sections 1.2.5 and 3.2.6).

In the COMfort FormulA model (COMFA) (sections 1.2.3 and 3.2.6), even though T_{mrt}, per se, is not an input, absorbed radiation (R_{abs}), i.e. radiant load, is estimated within the COMFA model itself from outputs of down-welling and outgoing short- and longwave fluxes of the SOLWEIG model.

3.2.6 THERMAL COMFORT INDICES

In **Paper IV** thermal comfort is estimated for 5 year old boys that are 111.15 cm long and weigh 19.6 kg. The length and weight are determined from averages of 5 year old boys according to Albertsson Wikland et al. (2002). Estimations are made for boys because of their slightly higher metabolic heat production (Schofield, 1985). This information is used in two thermal comfort indices: COMFA and PET.

COMFA is estimated with the updated model by Cheng and Brown (2020), referred to as COMFA-kid. Here, a threshold to determine heat stress is set to 80 Wm^{-2}, indicating "Too warm" conditions (Cheng and Brown, 2020). For PET a threshold of 29 °C PET is used in the analysis to determine moderate heat stress (Matzarakis et al., 1999). An additional thermal comfort index, UTCI, is used in **Paper IV** with a threshold of 26 °C to determine moderate heat stress (Blazejczyk et al., 2010). Here, however, human energy balance is always estimated for an adult (see section 1.2.5).

3.2.7 FIELD MEASUREMENTS

The parameterization scheme for longwave radiation (**Paper II**) is evaluated using observations of short- and longwave radiation fluxes from Guldhedstorget, a square next to the Department for Earth Sciences, University of Gothenburg. The field observations were conducted following the method by Höppe (1992) with the corrections by Holmer et al. (2015), and accordingly short- and longwave fluxes and T_{mrt} are estimated on a human represented by a cylinder. Measurements were conducted using three Kipp & Zonen CNR1 Net Radiometers (Kipp & Zonen, 2009) and one Delta-T SPN1 Sunshine Pyranometer (Wood, 2019).

3.3 DOWNSCALING OF REGIONAL CLIMATE MODEL SIMULATIONS

3.3.1 REGIONAL CLIMATE MODEL SIMULATIONS

In **Paper IV** six regional climate model (RCM) simulations from the EURO-CORDEX project (Vautard et al., 2013; Kotlarski et al., 2014) are used, all downscaled with the SMHI Rossby Center RCA4 RCM (Samuelsson et al., 2011; Nikulin et al., 2011). RCM simulation data from the EURO-CORDEX have relatively high spatial and temporal resolution and are openly available. The RCA4 RCM is forced with the GCMs given in table 1. These simulations are, in turn, statistically downscaled for five locations in Sweden, Malmö, Gothenburg, Stockholm, Östersund and Luleå, with the methods described in section 3.3.2.

*Table 1. EURO-CORDEX driving models and experiments, downscaled with the SMHI Rossby Center RCA4 RCM. All model experiments are from the r1i1p1 ensemble except ICHEC-EC EARTH, which are from the r12i1p1 ensemble (modified table x from **Paper IV**).*

Model	Historical	RCP 2.6	RCP 4.5	RCP 8.5
CNRM-CERFACS-CNRM-CM5 (Voldoire et al., 2012)	x		x	x
ICHEC-EC-EARTH (Hazeleger et al., 2011)	x	x	x	x
IPSL-IPSL-CM5A-MR (Dufresne et al., 2013)	x		x	x
MOHC-HadGEM2-ES (Collins et al., 2011)	x	x	x	x
MPI-M-MPI-ESM-LR (Giorgetta et al., 2013)	x	x	x	x
NCC-NorESM1-M (Tjiputra et al., 2013)	x	x	x	x

Three representative concentration pathways (RCP) are used. RCP2.6, referred to as peak-and-decay, represents a climate change scenario where radiative forcing is peaking by the mid-century after which it decreases and eventually reaches 2.6 Wm^{-2} by 2100. In RCP4.5, a midrange mitigation emissions scenario, radiative forcing continues to increase until it stabilizes at 4.5 Wm^{-2} by the end of the century, whereas RCP8.5, a high emission scenario, will reach

8.5 Wm^{-2} by 2100 and continue to increase (Moss et al., 2012; Taylor et al., 2012).

3.3.2 DOWNSCALING ALGORITHM

In **Paper IV** the aim was to study thermal comfort of preschoolers in five Swedish cities in a future climate. However, openly available output data from most RCMs simulating future climate scenarios have relatively coarse spatial resolution (0.11° for model simulations in the EURO-CORDEX project (Vautard et al., 2013; Kotlarski et al., 2014)) and temporal resolution (daily averages). However, when studying thermal comfort of preschoolers it is preferred to have at least hourly temporal resolution and a spatial resolution representative to a city, neighborhood or street, to make any reasonable assumptions on temporal changes and effects of the surrounding surfaces and geometries. One way of obtaining hourly resolution meteorological data for a city located within a 0.11° pixel is through statistical downscaling.

Rayner et al. (2014) presented a method to statistically downscale future T_{air} and G from RCM simulations by using change factors (CF) on observed data. In their method, CF between a simulated historical period, covering a period where observations are also available, and a simulated future period are applied to the observed data. In this way the observed data can be used to depict a current climate and modified to represent a future climate. Moreover, it is possible to avoid biases in climate model simulations, i.e. where a historical period have either lower or higher T_{air} compared to observations for the same period.

The method by Rayner et al. (2014) works well in estimations of future T_{mrt} as it downscales T_{air} and G, and is used accordingly. However, thermal comfort indices like COMFA, PET and UTCI, used in **Paper IV**, require RH and WS as input. Therefore, a new downscaling algorithm had to be developed for estimation of future RH and WS. While RH is sensitive to temperature, specific humidity is rather consistent throughout a day. Therefore, specific humidity (huss) is downscaled. From this CF of specific humidity for deciles of maximum T_{air} are estimated. Same method is used for WS. An example is given in the following page for observed specific humidity (2008-2020) and two simulation periods, 2001-2030 (historical) and 2071-2100 (future):

1. Observations are available for 2008-2020.

2. A base period is determined in the historical RCM simulation from which a future CF will be calculated: 2001-2030. This period covers the observation period.

3. A period is decided for the future RCP8.5 simulation: 2071-2100.

4. Retrieve time steps (days) when maximum T_{air} is within 0–10th percentile in both historical (2001-2030) and future simulations (2071-2100). Obtain specific humidity for the corresponding time steps.

5. Estimate the CF between the historical and future periods using the median of both periods

$$CF = median(future\ huss)/median(hist\ huss)$$

6. Apply CF on observed specific humidity (2008-2020) for days when observed daily maximum T_{air} is with 0-10th percentile.

7. Estimate and apply CF for 10-20th percentile and the remaining percentile bands (step 4-6).

An example from 2019-07-26 of what the meteorological data on this day would look like in 2071-2100 with the downscaling algorithms used here is depicted in figure 3. It is evident that T_{air} (fig. 3a) is subject to largest change, particularly under RCP8.5, which influences radiant load (fig. 3e) and in turn COMFA (fig. 3f).

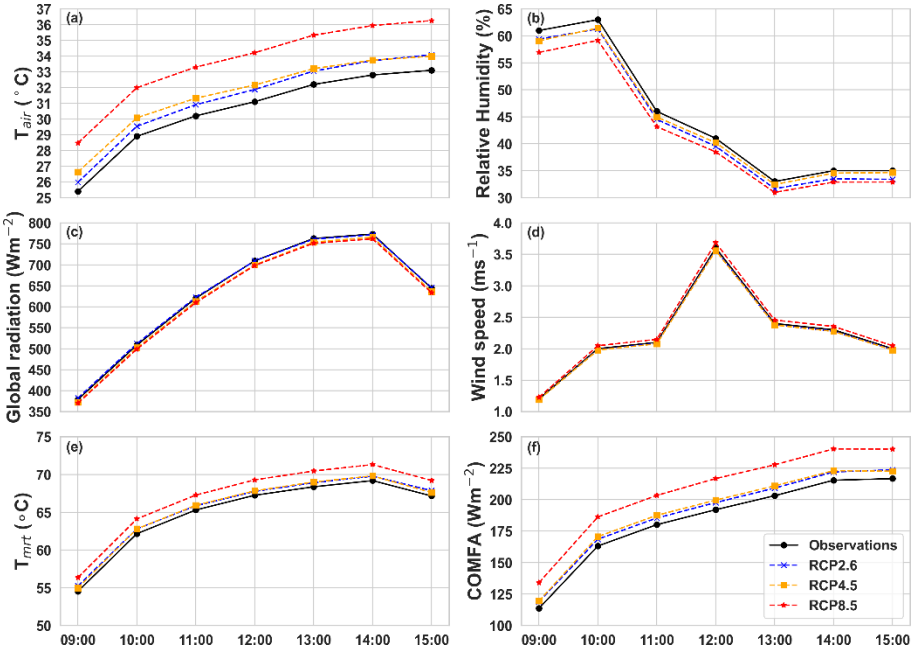

Figure 3. Graphs showing observed (2019-07-26) and future (2071-2100 under RCP2.6, 4.5 and 8.5) air temperature (T_{air}), relative humidity, global radiation, wind speed, mean radiant temperature (T_{mrt}) and COMFA, in Gothenburg. Future values of RH and WS are estimated with the downscaling algorithm. Future T_{air} and global radiation are estimated following the methods by Rayner et al. (2014).

3.4 ALGORITHMS IN TREEPLANTER

In **Paper V** a tool (TreePlanter) to determine tree locations for optimal shading effect and mitigation of radiant load based on output T_{mrt} and shadow patterns from SOLWEIG is presented. The tool utilizes two metaheuristic algorithms: a hill-climbing and a greedy algorithm.

Finding optimal locations for multiple trees is a computationally extensive procedure. As an example, a gridded area with

$$n = 500$$

possible locations for trees, where optimal positions for

$$k = 5$$

trees are studied, would require

$$\frac{\mathrm{n!}}{\mathrm{(n-k)!k!}} = 2.5 * 10^{11}$$

brute-force calculations, considering all possible combinations. Metaheuristics is a way to avoid brute-force calculations, but still find suitable solutions within limited time or with limited computational power (Luke, 2013). Here, output T_{mrt} and shadow patterns from SOLWEIG for given time steps are used to create a grid with estimated difference in T_{mrt} between sunlit and shaded (by a tree and estimated with the 1D version of SOLWEIG) conditions for each possible position using one tree. The difference in T_{mrt} is the mitigating effect. This grid is explored using a hill-climbing algorithm that step-wise moves two or more trees, one at a time (number of trees are determined by the user), to locations where the mitigating effect is higher for the studied time steps.

The greedy algorithm ranks the mitigating effect of all possible locations and determines tree positions according to the ranking.

The concept in both algorithms is essentially that the mitigating effect is estimated for all possible locations using one tree. The algorithms then adjusts for potentially overlapping tree shadows from the moving trees. This substantially decreases the number of calculations required in comparison to a brute-force approach.

3.5 INTERVIEWS WITH PRESCHOOL PERSONNEL

Paper III include semi-structured interviews with preschool teachers, conducted in spring 2019. In total 19 interviews were completed with teachers from 19 different preschools in Gothenburg, Sweden. The interviews were conducted to investigate how heat stress events are experienced by the teachers and affects the preschool children, their activities and possible heat mitigating actions.

4 RESULTS AND DISCUSSION

4.1 MODELLING ANISOTROPIC SHORT- AND LONGWAVE RADIATION

When studying urban climate and variables important for the human energy balance, e.g. T_{mrt}, using computer simulations, it is important that the models can capture and depict as much of reality as feasible. This is not always possible as some processes may be too small-scale or complex to solve in relation to e.g. spatial or temporal resolution of the model. Instead, such processes can be parameterized, i.e. simplified.

4.1.1 PARAMETERIZATION OF SKY DIFFUSE SHORTWAVE RADIATION

The implementation of the SRA (Robinson and Stone, 2004; 2005), based on the All-weather model for sky illuminance distribution (Perez et al., 1993) and division of the sky-vault into 145 patches (Tregenza, 1987), presented in **Paper I**, showed that radiant load is higher in front of sunlit facades exposed to the circumsolar brightening (McArthur & Hay, 1981). Shaded areas, on the other hand, had lower T_{mrt}. It has been shown in previous studies, utilizing isotropic skies, that areas close to sunlit facades are exposed to high radiant load because of the exposure to shortwave (solar) radiation and high longwave irradiance from surrounding sunlit surfaces (Lindberg et al., 2014; Thorsson et al., 2017). The results from **Paper I** indicate that radiant load in these areas are actually even higher if an anisotropic sky is considered. The increased exposure is explained first and foremost by the circumsolar brightening, where more diffuse shortwave originates from the area close to the solar disc (McArthur & Hay, 1981), but also by the horizon brightening. As indicated by the results (fig. 4) radiant load is higher in March (fig. 4e) compared to June (fig. 4b). This is explained by a lower solar altitude in March (fig. 4f), resulting in the circumsolar brightening being almost perpendicular to the vertical of human, thus increasing the intensity of radiation, hence increasing the radiant load with a resulting increase in T_{mrt} up to 3 °C. The decreased exposure to the circumsolar brightening in shaded areas resulted in an up to 1.2 °C and 1.7 °C lower estimated T_{mrt} for June and March, respectively. Evaluations by Lindberg and Grimmond (2011) and Kántor et al. (2018) showed

overestimations of T_{mrt} in shaded areas. Moreover, Kántor et al. (2018) showed that SOLWEIG underestimated T_{mrt} in sunlit areas.

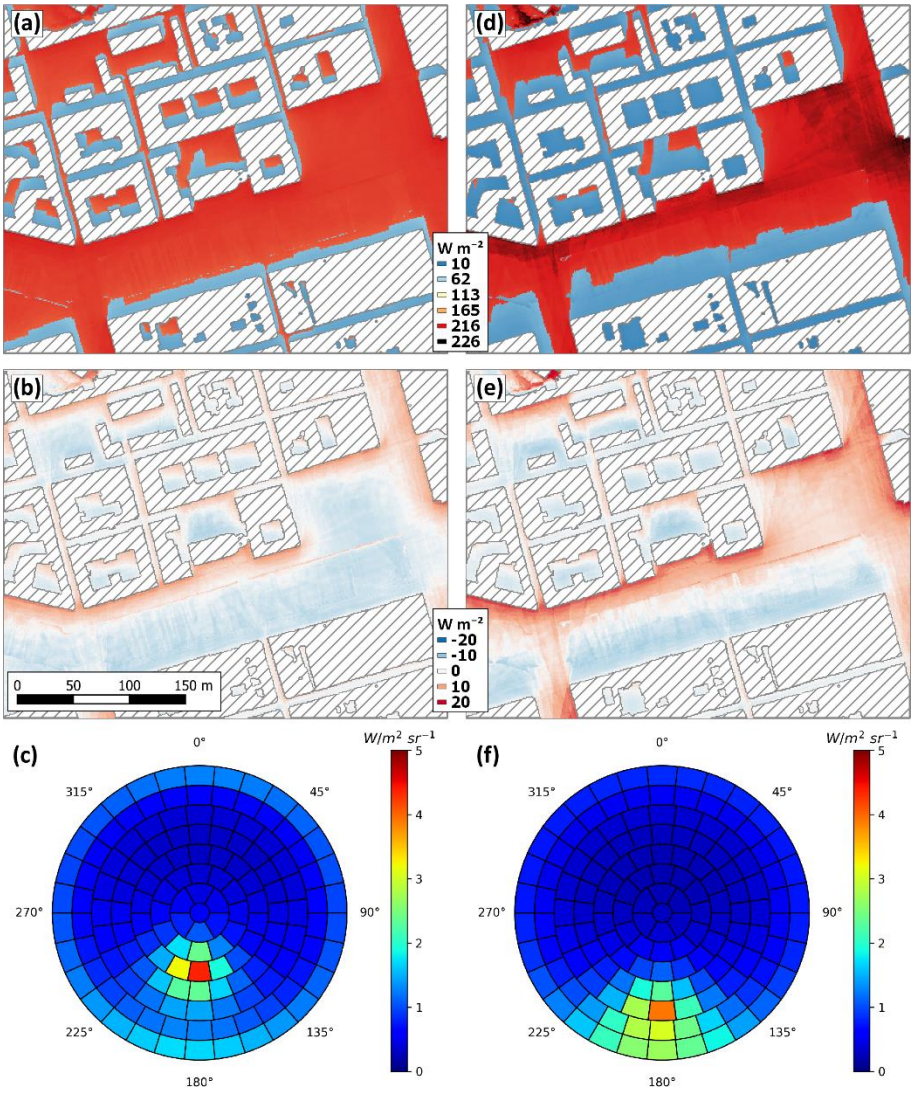

*Figure 4. K_{tot} received by a standing human represented by a cylinder (1200 h LST 22 June 1983; G = 822.4, I = 844.7, D = 125.3 W m^{-2}) with (a) an anisotropic sky for diffuse radiation for summer solstice, (b) difference between (a) and K_{tot} with an isotropic sky for diffuse shortwave radiation at the same time, and (c) the corresponding anisotropic sky vault. Figs. (d-f) show the same information as in (a-c) but for spring equinox (1200 h LST 20 March 1984; G = 541.5, I = 798.0, D = 110.5 W m^{-2}). Dashed areas represent buildings (modified from figure 3 in **Paper I**).*

The results from **Paper I** and the over- and underestimations from previous studies indicates improvements in simulations of the shortwave component by SOLWEIG.

4.1.2 PARAMETERIZATION OF LONGWAVE RADIATION

The parameterization scheme for longwave radiation is evaluated with field measurements on Guldhedstorget, Gothenburg (fig. 5). The evaluation of the new model revealed an overestimation of longwave radiation for directions where building surfaces are visible.

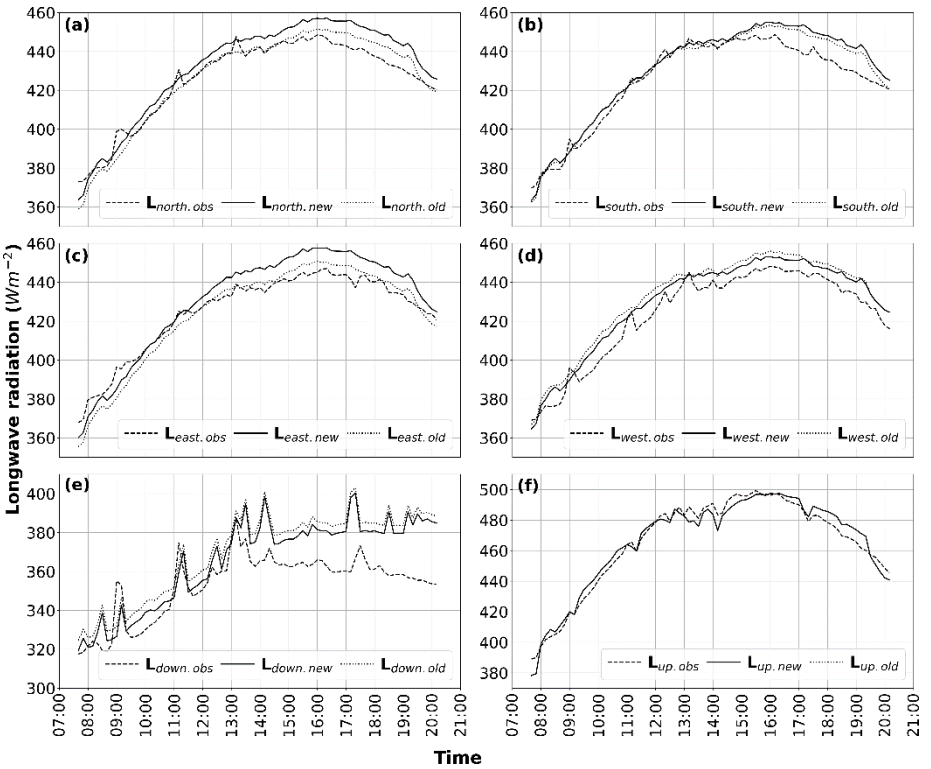

*Figure 5. Six directional observed and simulated longwave radiation data (10 min resolution) for a relatively clear day (2021-06-17). The figure show longwave radiation fluxes from (a) north, (b) south, (c) east, (d) west, (e) upper hemisphere and (f) ground. Dashed lines depicts observed values. Solid and dotted lines represent the new and old parameterization schemes, respectively (figure 4 in **Paper II**).*

These overestimations are most noticeable when these building surfaces are sunlit, indicating that they are associated with the parameterization scheme for

sunlit surfaces rather than the parameterization scheme for longwave radiation, i.e. the patches. This is best exemplified in fig. 5d, where longwave fluxes from west are shown. Here, the new and the old parameterization scheme show similar results. In fig. 5c, on the other hand, longwave radiation originating from east is depicted. In this direction there is no vegetation and some of the building surfaces in this direction are sunlit already in the morning, whereas some become sunlit in early afternoon and stay sunlit until sunset. If building surfaces are sunlit using the old parameterization scheme for longwave radiation, such surfaces are always located at the top of building walls (Lindberg et al., 2008). In the new scheme, on the other hand, sunlit surfaces can reach ground level. This means that if the surface temperature of sunlit surfaces is overestimated, emitted longwave radiation from these surfaces will have less impact on T_{mrt} when such surfaces are located at the top of a building compared to the new scheme where sunlit surfaces can be perpendicular to the vertical of a human.

An output from SOLWEIG (figure 6) show that T_{mrt} is up to 1-1.5 °C higher in open areas (figure 6d) with the anisotropic sky (figure 6a) compared to if an isotropic sky (figure 6b) is utilized. Similar to the exposure to the circumsolar brightening in **Paper I**, exposure to the lower parts of the sky-vault increases radiation received on the vertical of a human and hence increases radiant load.

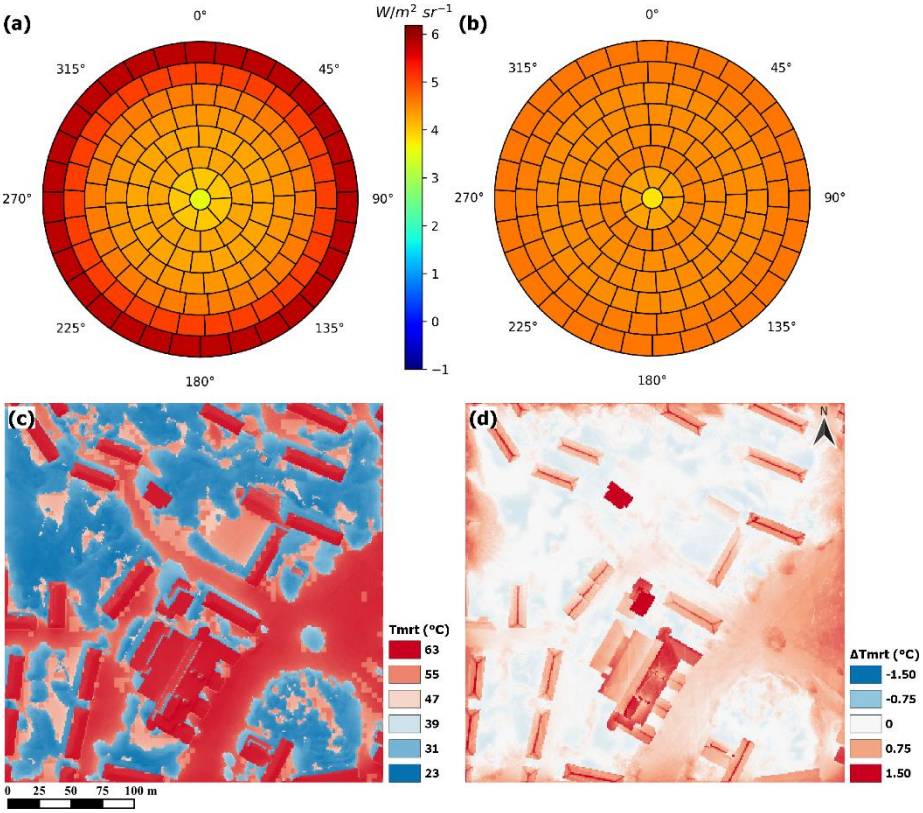

*Figure 6. Figure showing output from SOLWEIG for 2021-06-17 12:10 LST, where (a) shows longwave irradiance from an anisotropic sky and (f) from an isotropic sky, normal to a surface. Figure (c) shows T_{mrt} for a human represented by a cylinder with an anisotropic sky for longwave radiation and (d) the difference in T_{mrt} (cylinder) for the corresponding time with an isotropic sky (anisotropic sky – isotropic sky) (figure 8 in **Paper II**).*

4.1.3 ANISOTROPIC SHORT- AND LONGWAVE RADIATION

Figure 7 show the difference in T_{mrt} when running SOLWEIG with the new parameterization schemes and the old approach using SVF. Here, it is evident that T_{mrt} underneath trees (dark blue areas) have declined substantially (up to 7 °C) as an effect of these areas being blocked by the circumsolar brightening (**Paper I**), and improved parameterization of longwave fluxes (**Paper II**). Gal and Kántor (2020), in an extensive radiation model evaluation, showed overestimations in SOLWEIG of T_{mrt} underneath trees by up to 7 °C, indicating that results shown here are in the right direction. There are also increases in T_{mrt} in front of sunlit facades (up to 4 °C), which needs to be further addressed and evaluated, considering the possible overestimations from sunlit walls.

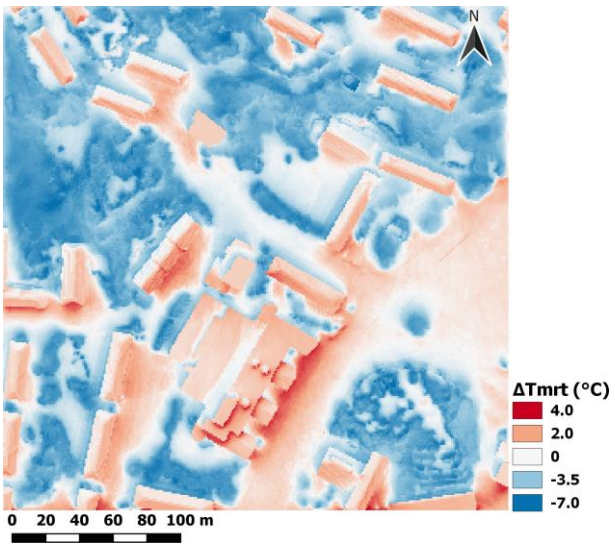

Figure 7. Map showing difference in mean radiant temperature (T_{mrt}) between new and old versions of SOLWEIG for 2021-06-17 12:10 LST. In the new version of SOLWEIG sky diffuse shortwave radiation and longwave radiation originating from the upper hemisphere has been divided into 153 patches compared to the old version of SOLWEIG where these fluxes are estimated from sky view factors. Positive values indicate larger T_{mrt} with the new version of SOLWEIG and negative values demonstrate areas where T_{mrt} is lower.

The results from **Papers I** and **II** indicates that anisotropic skies for diffuse shortwave radiation and longwave radiation are important in estimations of radiant load. In addition to this, directionality is important, as depicted in **Paper II**.

4.2 THERMAL COMFORT OF PRESCHOOLERS IN THE PRESENT AND FUTURE CLIMATE

Children are vulnerable to heat (see section 1.4). Moreover, there are general recommendations that they spend time outdoors in the preschool yard, which is a confined area that the children in general are not allowed to leave. This makes it imperative to study the possible effects of climate and weather on their wellbeing. The following subsection gives overviews of **Papers III** and **IV**, where thermal comfort of preschoolers in a present climate and future climate are studied.

4.2.1 OUTDOOR THERMAL COMFORT OF PRESCHOOLERS IN THE PRESENT CLIMATE

The results from **Paper III** revealed unpleasant preschool yard conditions. Two thirds of the 440 studied preschools in Gothenburg had 50% or more of their yards exposed to strong heat stress on hot and clear days. It is disclosed from interviews with preschool personnel that such conditions have negative consequences for the children. Not only do the children get drowsy, tired and overheated, but pedagogical activities are hindered. Instead of focusing on pedagogical activities, teachers have to put their attention to care, ensuring that the children do not overheat. Malmquist et al. (2021) came to similar conclusions in their study on preschoolers in Linköping, Sweden. Interviews conducted by Malmquist et al. (2021) even revealed that some children, during hot weather events, were on the brink of fainting. Results from SOLWEIG simulations in **Paper III** showed that high T_{mrt} correlated with low amount of shade (fig. 8a) and low amount of trees (fig. 8b). Low radiant load, thus, corresponds with high amount of shade and high amount of shade corresponds with high fraction of trees (fig. 8c). Interviewees also supported this, where those in exposed preschool yards had more heat related problems compared to those in preschools with access to shade. Interviewees also indicated that shading from trees is favored compared to artificial shading from e.g. shading sails and parasols.

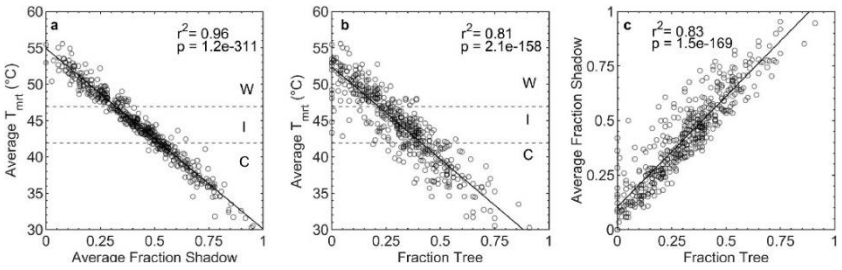

*Figure 8. Correlation between average Tmrt for 1 June 2018, 11:00-15:00 and a) average fraction of shadow, b) fraction of tree, and c) correlation between fraction tree and average fraction shadow (figure 6 in **Paper III**).*

Simulated thermal comfort of preschoolers, presented in **Paper IV**, likewise, showed that there are severe risks already in the present climate. Results show that number of days when preschoolers are at risk of moderate to strong heat stress all hours 09:00-15:00 May through August exceed 10 in Malmö, Gothenburg and Stockholm (fig. 9), when playing in a sunlit sandbox, regardless of thermal comfort index. Östersund and Luleå have fewer heat stress days, with Luleå having twice the number of days compared to Östersund.

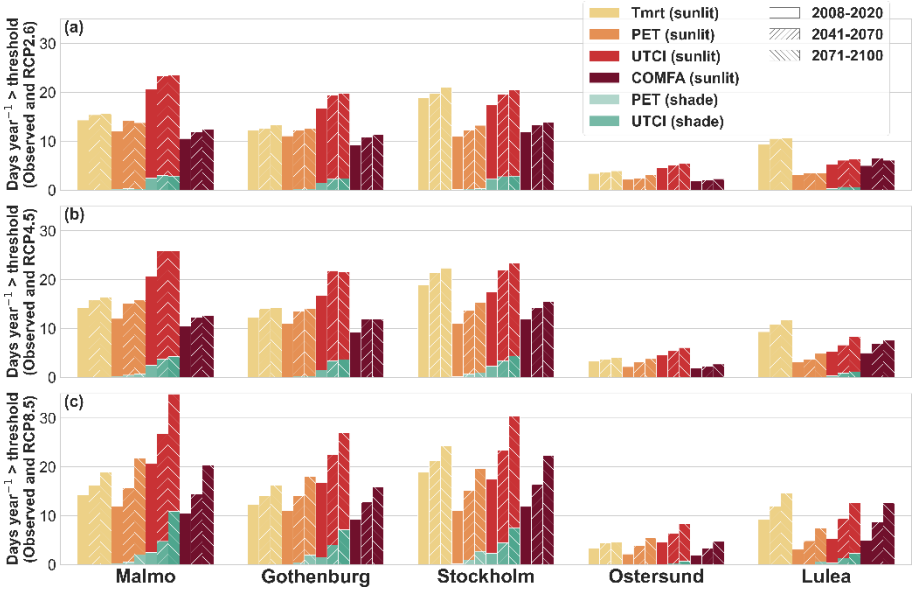

*Figure 9. Days year^{-1} when all hours between 09:00 and 15:00 May through August are above 52 °C T_{mrt}, 29 °C PET, 26 °C UTCI or 80 Wm^{-2} COMFA, for (a) RCP2.6, (b) RCP4.5 and (c) RCP8.5, in sunlit and shaded conditions. Estimations are made for observations (2008-2020) and two future periods, 2041-2070 and 2071-2100, under the RCP2.6, 4.5 and 8.5 scenarios (modified from figure 4 in **Paper IV**).*

4.2.2 OUTDOOR THERMAL COMFORT OF PRESCHOOLERS IN A FUTURE CLIMATE

When thermal comfort of Swedish preschoolers is analyzed for future climates (**Paper IV**), the results indicate that climate change will increase already pressing problems, although future changes depend on climate change scenario. Under the RCP2.6 scenario changes are small, yet some increases can be seen for T_{mrt} and all thermal comfort indices by the end of the century (fig. 9a). Increases in days per year with moderate to strong heat stress under the RCP4.5 scenario are more evident (fig. 9b), whereas days $year^{-1}$ under the RCP8.5 scenario show large increases (fig. 9c), especially in Malmö, Gothenburg and Stockholm. Here number of days with strong heat stress have increased by a factor 1.5-2 for all variables and all locations under the worst case scenario (fig. 9c).

Paper IV indicated discrepancies between thermal comfort indices when active play (more intense activity) was simulated (not shown). COMFA has the advantage that it is sensitive to changes in physiological characteristics and activities. PET, on the other hand, is a good estimator of heat stress during sedentary activities. During more intense activities, such as intense play, however, differences in PET are small, leading to underestimations of thermal comfort conditions compared to COMFA. Similar conclusions have been drawn from previous studies (Liu & Jim, 2021). With UTCI, on the other hand, it is not possible to analyze more intense activities since this index is based on a linear relationship of T_{air}, T_{mrt}, RH and WS, with physiological characteristics being incorporated (Blazejczyk et al., 2010). Moreover, UTCI is developed for adults. This indicates the importance of appropriate thermal comfort indices in applied studies, where indices like PET and UTCI are valuable in studies on exposure to heat stress during sedentary activities, while COMFA is recommended in thermal comfort studies during activities more intense than sedentary, e.g. running. The results from simulated play in a sandbox and active play, with COMFA, are given in table 2.

Present climate conditions show that Malmö, Gothenburg and Stockholm (and to some extent Luleå) have several days per year, May through August, where all hours 09:00-15:00 are determined too hot (table 2) according to COMFA (Cheng and Brown, 2020), even during calm activities such as playing in a sandbox, in sunlit conditions. In Stockholm, which is one of the hottest

locations in **Paper IV**, children playing in preschool yards similar to the one depicted in the study are subject to almost a full week of heat stress in July alone. If the children are running around heat stress days amount to almost a month per year, where July is most pronounced, although many days occur in May, June and August as well. If, on the other hand, shading is provided, heat stress days are almost entirely diminished.

The analysis of future climate scenarios (table 2) show that number of heat stress days in Malmö, Gothenburg, Stockholm and Luleå have increased to more than a week per year for children playing in sunlit sandboxes, in July alone, under the highest emission scenario (RCP8.5). In Stockholm there is a sum of around 2.5 weeks per year with strong heat stress days in July and up to 7 weeks, May through August, for intense activities. Again, mitigation

*Table 2. Days year^{-1} when COMFA is > 80 Wm^{-2} all hours 09:00-15:00 in May, June, July and August (M, J, J, A) when playing in sandbox (MET = 2.23) and active play (MET = 4.16) in sunlit and shaded conditions for Luleå, Östersund, Stockholm, Gothenburg and Malmö for 2008-2020 (observations), 2041-2070 (RCP2.6, 4.5 and 8.5) and 2100 (RCP2.6, 4.5 and 8.5) (table 6 in **Paper IV**).*

	Sandbox (sunlit)				Sandbox (shade)				Active (sunlit)				Active (shade)			
Luleå																
Observ. 2008-2020	0.2	1.2	3.3	0.3	0.0	0.0	0.0	0.0	1.3	3.6	8.2	2.9	0.0	0.1	0.2	0.0
RCP2.6 2041-2070	0.5	1.3	4.4	0.4	0.0	0.0	0.0	0.0	1.5	4.4	9.5	3.2	0.0	0.1	0.5	0.2
2071-2100	0.5	1.3	4.0	0.3	0.0	0.0	0.0	0.0	1.5	4.4	9.4	3.0	0.0	0.1	0.5	0.1
RCP4.5 2041-2070	0.5	1.3	4.6	0.5	0.0	0.0	0.0	0.0	1.6	4.5	10.3	3.8	0.0	0.1	0.8	0.2
2071-2100	0.5	1.5	4.8	0.7	0.0	0.0	0.0	0.0	1.8	5.4	11.0	4.5	0.0	0.1	1.2	0.2
RCP8.5 2041-2070	0.6	1.7	5.5	0.8	0.0	0.0	0.0	0.0	1.8	5.5	11.3	4.8	0.0	0.1	1.2	0.2
2071-2100	0.7	2.8	7.4	1.8	0.0	0.0	0.0	0.0	2.1	7.9	13.4	6.3	0.0	0.3	2.5	0.2
Östersund																
Observ. 2008-2020	0.2	0.5	1.3	0.0	0.0	0.0	0.0	0.0	0.5	2.5	3.8	0.6	0.0	0.0	0.0	0.0
RCP2.6 2041-2070	0.1	0.5	1.4	0.0	0.0	0.0	0.0	0.0	0.7	2.7	4.2	0.8	0.0	0.0	0.0	0.0
2071-2100	0.1	0.7	1.5	0.0	0.0	0.0	0.0	0.0	0.6	2.9	4.1	0.8	0.0	0.0	0.0	0.0
RCP4.5 2041-2070	0.1	0.5	1.6	0.0	0.0	0.0	0.0	0.0	0.8	2.9	4.5	0.8	0.0	0.0	0.0	0.0
2071-2100	0.2	0.7	1.8	0.0	0.0	0.0	0.0	0.0	1.2	3.2	4.8	1.1	0.0	0.0	0.0	0.0
RCP8.5 2041-2070	0.2	1.0	2.2	0.1	0.0	0.0	0.0	0.0	1.2	3.5	4.7	1.2	0.0	0.0	0.0	0.0
2071-2100	0.2	1.5	2.8	0.2	0.0	0.0	0.0	0.0	1.5	4.5	6.3	1.8	0.0	0.0	0.2	0.0
Stockholm																
Observ. 2008-2020	1.1	3.7	6.0	1.1	0.0	0.0	0.0	0.0	3.8	10.0	12.4	6.2	0.0	0.1	1.3	0.2
RCP2.6 2041-2070	1.3	3.8	6.8	1.5	0.0	0.0	0.0	0.0	4.4	10.5	13.8	7.5	0.0	0.1	2.1	0.2
2071-2100	1.2	3.9	7.1	1.7	0.0	0.0	0.0	0.0	4.2	11.2	13.8	7.5	0.0	0.2	2.2	0.2
RCP4.5 2041-2070	1.5	3.8	7.2	1.6	0.0	0.0	0.0	0.0	4.8	11.1	14.5	7.8	0.0	0.3	2.4	0.2
2071-2100	1.6	4.1	7.8	2.0	0.0	0.0	0.0	0.0	5.4	11.8	14.9	8.5	0.0	0.5	2.5	0.2
RCP8.5 2041-2070	1.5	4.9	7.7	2.3	0.0	0.0	0.0	0.0	4.8	12.1	14.7	8.5	0.0	0.5	2.5	0.2
2071-2100	2.1	7.0	9.9	3.3	0.0	0.0	0.1	0.0	5.8	13.2	17.3	12.1	0.0	1.6	4.3	1.0
Gothenburg																
Observ. 2008-2020	0.8	3.2	4.8	0.5	0.0	0.0	0.0	0.0	3.3	7.6	9.5	3.5	0.0	0.2	0.6	0.0
RCP2.6 2041-2070	0.9	3.1	5.9	0.9	0.0	0.0	0.0	0.0	3.5	7.6	10.8	4.2	0.0	0.2	0.8	0.0
2071-2100	0.8	3.5	6.1	1.0	0.0	0.0	0.0	0.0	3.5	8.0	10.8	4.4	0.0	0.2	0.8	0.0
RCP4.5 2041-2070	1.0	3.7	6.2	0.9	0.0	0.0	0.0	0.0	4.1	8.3	11.2	4.5	0.1	0.2	1.3	0.0
2071-2100	1.1	3.8	6.2	0.8	0.0	0.0	0.0	0.0	4.4	8.7	11.3	4.8	0.1	0.3	1.6	0.1
RCP8.5 2041-2070	1.1	4.2	6.2	1.3	0.0	0.0	0.0	0.0	4.0	8.7	11.3	5.0	0.1	0.5	1.6	0.2
2071-2100	1.5	5.2	7.2	2.0	0.0	0.0	0.0	0.0	5.2	10.5	12.8	7.2	0.2	1.0	3.7	0.5
Malmö																
Observ. 2008-2020	0.4	3.2	5.7	1.3	0.0	0.0	0.0	0.0	4.3	9.2	10.5	6.2	0.0	0.2	0.9	0.2
RCP2.6 2041-2070	0.5	3.3	6.6	1.4	0.0	0.0	0.0	0.0	4.5	9.6	11.8	7.1	0.0	0.3	1.4	0.2
2071-2100	0.5	3.7	6.9	1.4	0.0	0.0	0.0	0.0	4.4	10.0	11.9	6.8	0.0	0.3	1.2	0.2
RCP4.5 2041-2070	0.5	3.7	6.6	1.4	0.0	0.0	0.0	0.0	4.8	10.2	12.0	7.5	0.0	0.4	1.5	0.3
2071-2100	0.5	3.8	6.9	1.5	0.0	0.0	0.0	0.0	5.1	10.4	12.4	7.7	0.0	0.5	1.8	0.3
RCP8.5 2041-2070	0.5	4.8	7.2	2.0	0.0	0.0	0.0	0.0	4.7	10.7	12.1	8.5	0.0	0.5	1.8	0.4
2071-2100	1.2	6.3	8.9	4.0	0.0	0.0	0.0	0.0	6.2	12.2	14.5	10.8	0.1	1.6	4.2	1.5
	M	J	J	A	M	J	J	A	M	J	J	A	M	J	J	A

Days year^{-1} (COMFA > 80 Wm^{-2})

by tree shade show great potential, reducing the numbers to around or less than a week per year by the end of the century under RCP8.5.

Future increases in heat stress days, disclosed in **Paper IV**, will likely exacerbate the problems described in **Paper III** where hot days result in tired, drowsy and overheated children, with negative consequences for learning and pedagogical activities. Moreover, the risk of negative effects on the wellbeing and health of children will increase, e.g. fainting as described by Malmquist et al. (2021). The results from **Papers III** and **IV** clearly demonstrate the importance of sufficient shading in preschool yards to reassure a safe environment where the children are not at risk of overheating, heat stroke and dehydration (Kovats & Hajat, 2008).

4.3 MITIGATING EXCESSIVE RADIANT LOAD

As demonstrated in **Papers I**, **II**, **III** and **IV** exposure to heat stress is influenced by exposure shortwave radiation. Trees are regularly recommended as an option to mitigate excessive radiant load in exposed areas (Konarska et al., 2014; Vanos et al., 2017; Lee & Mayer, 2020). The potential of trees to mitigate heat and increase thermal comfort is exemplified in **Papers III** and **IV**. Nevertheless, few studies address optimization when positioning trees to mitigate heat.

In **Paper V**, TreePlanter, a tool to optimize tree locations to mitigate radiant load is presented. The initial idea was to see if two or more trees could shade same area as one tree but with their combined shadows, i.e. from more optimized locations, where their shade would also affect other ground surfaces. While this is the case (although not shown here), the results were not extraordinary for the study area (Järntorget in the central parts of Gothenburg, Sweden). Nevertheless, the results from simulations showed that tree size and number of trees can be of importance when planning to mitigate radiant load in an area. An example is given in figure 10, where the black circles in figure 10a, 10c and 10d show locations for five trees determined by the tool with the hill-climbing algorithm. In figure 10a the trees are 5 m high with a 3 m canopy diameter and 2 m trunk zone (distance from ground to canopy). Tree sizes in figure 10c and 10d are 8 m (height), 5 m (canopy diameter) and 2 m (trunk zone) and 12 m (height), 7 m (canopy diameter) and 3 m (trunk zone), respectively. Most trees end up shading areas in front of sunlit facades, which

are known from previous studies as exposed to strong radiant load on clear and hot days (Thorsson et al., 2011; Lindberg et al., 2016; **Paper I**). As illustrated in the figure tree sizes influences the locations of the trees. For example, a juvenile tree (demonstrated by fig. 10a) provide shade from different locations than that of a mature tree (demonstrated by fig. 10c-d).

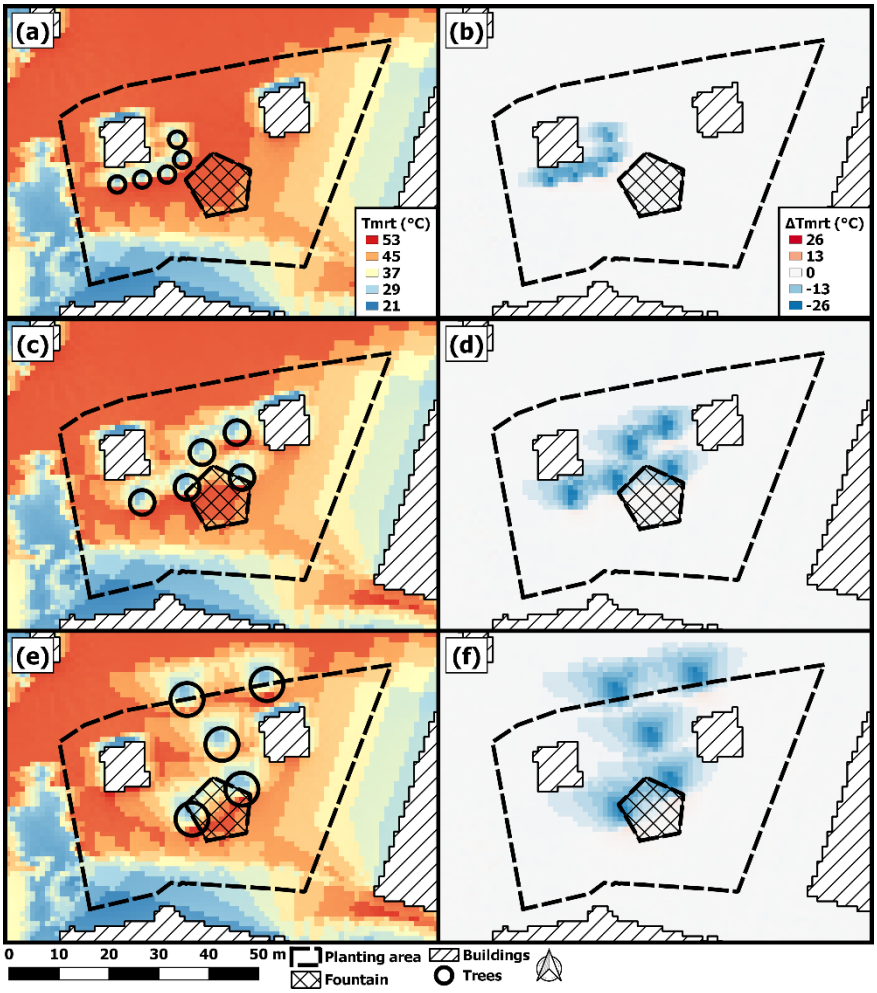

*Figure 10. Mean T_{mrt} for 09:00–16:00 LST on 22 June 1983, with locations of (a) five small trees, (c) five medium trees and (e) five large trees in black circles. Panels (b), (d) and (f) show corresponding differences in T_{mrt} between tree shade and sunlit areas for panels (a), (c) and (e), respectively (figure 4 in **Paper V**).*

It is also demonstrated that time of day, i.e. solar position, is decisive. An optimally positioned tree lead to a decrease in T_{mrt} of around 26 °C. Following

the linear relationship for PET and T_{mrt} by Mayer et al. (2008) and Lee et al. (2013) a decrease in T_{mrt} of 26 °C could result in a decrease in PET by around 13 °C, which could have immense effect on outdoor thermal comfort of humans.

The previous example (fig. 10) was created using a hill-climbing algorithm where the algorithm, step-wise, explores the grid for a better location where its corresponding tree shadow will have largest mitigating effect on radiant load. This process is relatively slow as it needs to adjust for potentially overlapping tree shadows. Another functionality in TreePlanter is to locate tree positions utilizing a greedy algorithm that ranks positions.

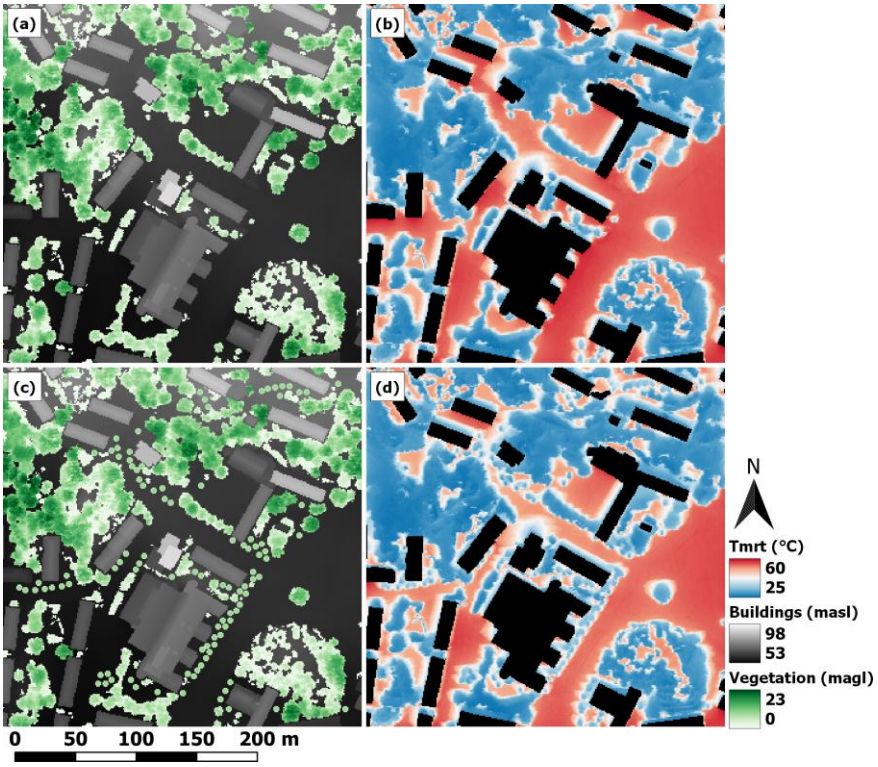

Figure 11. Maps showing (a) average T_{mrt} 11:00-14:50 on 2021-06-17, (b) a digital surface model (DSM) and canopy surface model (CDSM) used to estimate T_{mrt} in (a), (c) average T_{mrt} 11:00-14:50 on 2021-06-17 with 100 added trees using TreePlanter's greedy algorithm and (d) the corresponding DSM and CDSM.

This computationally faster function is exemplified in figure 11, illustrating an area around the Department of Earth Sciences, University of Gothenburg.

Figure 11b shows average T_{mrt} for 11:00-14:50 on 2021-06-17 with 10 minute time steps, which has been estimated using the DSM and CDSM depicted in figure 11a. In figure 11d T_{mrt} is averaged for the same period but with 100 new trees positioned using TreePlanter's greedy algorithm. Utilizing SOLWEIG output of T_{mrt} and shadow patterns for 11:00-14:50 calculated with the DSM and CDSM depicted in fig. 11a the greedy algorithm determines locations for 100 trees where the mitigating effect is evident (fig. 11d), mitigating high radiant load is the hottest areas illustrated in fig. 11b.

The drawback with TreePlanter is the computational time when the hill-climbing algorithm is applied. The alternative greedy algorithm is a valuable option in this sense, facilitating positioning of hundreds of trees in relatively low amount of time, as demonstrated in fig. 11, where locations for 100 trees were determined in around 20 minutes. There are, however, possibilities to improve computational speed, for example by running the tool on a graphics card (GPU). The results by Li and Wang (2021) are promising, showing great improvements in computational speed in calculations of SVF when running the SVF algorithm utilized in SOLWEIG on a GPU.

Other limitations relates to outdoor thermal comfort of humans that is influenced not only by T_{air} and T_{mrt} but also by RH and WS, which are not included in TreePlanter. Moreover, tree size and transmissivity of shortwave radiation through the tree canopy are fixed for all trees (although it is possible to changes it between model runs). Furthermore, T_{mrt} in the shade of the moving trees is estimated with the 1D version of SOLWEIG. Neither of the parameterization schemes presented in **Papers I** and **II** are utilized in **Paper V**, even though it now is possible. Nevertheless, considering that the 1D version is used and not the large version of SOLWEIG, longwave conditions underneath and around a tree do not include sunlit building surfaces in its vicinity, as it is estimated in an open area in the beginning of the model run.

To summarize, TreePlanter is a good complement to SOLWEIG in studies on urban planning and mitigation of radiant load in complex urban areas. As shown in the results locations for trees can differ depending on size and time of day.

4.4 SYNTHESIS

The implementation of anisotropic sky diffuse shortwave radiation and anisotropic longwave radiation together with the utilization of a patch system for the upper hemisphere have enabled a more realistic representation of the radiative characteristics in complex urban areas in SOLWEIG. The anisotropic sky for diffuse shortwave radiation (**Paper I**) is utilized in **Paper III** and it is possible to imagine that those preschools that are most exposed to strong radiant load would have had lower T_{mrt} without it. If the anisotropic longwave scheme had been ready and utilized simultaneously preschool yards at the cool end would likely have been even cooler considering that the cool preschool yards have abundant shade from trees.

In **Paper IV** anisotropic sky diffuse shortwave (**Paper I**) and anisotropic longwave radiation (**Paper II**) are applied. Here (**Paper IV**) the overestimations seen in the evaluation in **Paper II** are not as crucial, considering that the preschool yards in **Paper IV** are fictional. If the parameterization schemes had not been exploited in **Paper IV** radiant conditions and thermal comfort would have been different, especially in shaded conditions, where they would have been higher considering isotropic longwave radiation, potentially indicating more days with thermal discomfort.

Neither of the parameterization schemes in **Papers I** and **II** are utilized in **Paper V**. Nevertheless, optimal locations would likely still be in front of sunlit facades where the circumsolar brightening (**Paper I**) is realized. On the other hand, T_{mrt} under trees could potentially be even lower, but sunlit facades would not be included as T_{mrt} in the shade of the moving trees is estimated under a tree in an open area using the 1D version of SOLWEIG. This call for improvements of the TreePlanter tool to include estimations of T_{mrt} in tree shade using the 2D version of SOLWEIG.

5 CONCLUSIONS

Radiation models like SOLWEIG are essential in identifying areas that are exposed to heat stress during hot weather conditions. This is demonstrated in **Papers III** and **IV**, where two applied studies on preschoolers have increased our knowledge on the connection between the thermal microclimate in preschool yards and its possible effect on children. This also emphasizes the importance of skillful and fast models for accurate estimations of radiant conditions and continuation of model development. Even though there are some offsets in the model evaluation in **Paper II**, they are likely connected to the surface temperature scheme. Deviations close to sunlit buildings aside, improvements are evident considering sky diffuse shortwave radiation (**Paper I**), and sky longwave radiation and longwave radiation conditions under trees (**Paper III**). Without the improved radiant conditions under trees, thermal comfort would likely have been higher in the shaded preschool yard presented in **Paper IV**. The exposure to excessive radiant load and thermal discomfort in preschool yards described in **Papers III** and **IV** undeniably have negative effects on preschoolers. The TreePlanter tool, presented in **Paper V**, can be a valuable asset in urban planning, e.g. to position trees in a too hot preschool yard.

The objective of The Swedish National Expert Council on Climate Adaptation is to prepare a basis for the Swedish government in the continuation and future work on climate adaptation. This thesis, presented here, by all means, is a part of present and future climate adaptation in Sweden and elsewhere by its three parts consisting of model development, applications and mitigation. The model developments in **Papers I** and **II** reiterates the importance of continued model improvements. The applied studies in **Papers III** and **IV** demonstrate why we need models and the newly introduced tool in **Paper V** gives an example on how radiation models like SOLWEIG can be combined into new tools to be utilized in planning and design to mitigate excessive heat.

The main conclusions from this thesis are as follows:

- Realistic and accurate representation of short- and longwave radiation is important in modelling of radiant load in complex urban environments. The implementation of a model for anisotropic sky diffuse shortwave radiation means that

SOLWEIG now considers circumsolar and horizon brightening. Likewise, the implementation of a model for sky longwave radiation implies a more realistic representation of the sky-vault. Furthermore, the division of the sky-vault into 153 parts allows for directionality of radiation. An example of this is the improved and more realistic characteristics of radiant load under trees.

- Radiation models like SOLWEIG are important in applied studies analyzing heat stress in complex urban areas. This is demonstrated in both papers on preschoolers. Two thirds of preschool yards in Gothenburg, Sweden have 50% or more of their yard area exposed to heat stress on hot and clear days, already in the present climate. The negative consequences of hot weather are tired, drowsy and overheated children. Implications of tired, drowsy and overheated children is a shift from pedagogical activities to caregiving by preschool teachers.

- July is the hottest month analyzed, with almost two weeks of strong heat stress all hours 09:00-15:00 in Stockholm and Malmö, Gothenburg and Luleå close behind, already in the present climate. Such days are projected to increase to 2.5 weeks in Stockholm. Therefore, it is recommended that preschools remaining open in July have a large part of their outdoor area shaded.

- There is an increased risk of heat stress during hot weather on preschoolers in the future climate. In Malmö, Gothenburg and Stockholm, days per year with strong heat stress are projected to double in numbers under the RCP8.5 scenario, from approximately 10 to 20, when playing in a sunlit sandbox. Days and hours with thermal discomfort are even worse if more intensive activities are conducted such as running or energetic play.

- It is concluded both from simulations and from interviews with preschool personnel that trees and tree shade are important for the thermal comfort on preschool yards.

- Optimized tree positioning to mitigate excessive radiant load is essential. Optimal locations for trees can differ substantially depending the size of the trees and time of day when shading is necessary. TreePlanter is yet another tool that can help urban planners in decision making when designing and adapting urban areas to manage and mitigate excessive heat.

SOLWEIG and TreePlanter are open source and available in the Universal Multiscale Environmental Predictor (UMEP) toolbox (Lindberg et al., 2018) in QGIS (https://www.qgis.org).

6 FUTURE PERSPECTIVES

The results presented in this thesis manifests the vulnerability of children to heat (**Papers III** and **IV**). An additional group that requires further attention in its relation to heat in urban areas is the elderly population. Elderly are already identified as vulnerable to heat (Kovats & Hajat, 2008; Thorsson et al., 2014), although the connection to built-up areas and local and microclimate in a Swedish context is still relatively unexplored. Simulations of T_{mrt}, similar to the simulations in **Paper III**, should be appropriate to analyze the radiant conditions in the vicinity of e.g. elderly homes and areas frequented by the elderly population.

The TreePlanter tool, introduced in **Paper V**, is useful in urban planning and design for mitigation and adaptation to strong heat. Nevertheless, studies have indicated that mitigation of excessive heat in summer season can have the opposite effect in winter season when sunlight is desired (Konarska et al., 2014). A more comprehensive approach, analyzing changes in radiant load in all seasons, would give a more exhaustive interpretation of whether locations for trees are optimal or not. In addition to this, trees influences wind patterns and thermal comfort (Sjöman et al., 2015; Lee & Mayer, 2020), which demonstrates the importance of including wind in evaluations of optimized locations for trees. The URock model (Bernard et al., 2021) is a promising model for simulations of spatial wind patterns that will soon be available in the UMEP toolbox. It will enable spatial estimations of COMFA, PET and UTCI.

Other future work include an evaluation of the two new parameterization schemes (**Papers I** and **II**) in areas where spatial differences compared to the isotropic approach are large, e.g. under trees and close to sunlit walls. Field measurements close to sunlit walls would also include a thorough evaluation of the parameterization scheme for surface temperatures with possible improvements.

REFERENCES

Abdi, B., Hami, A. and Zarehaghi, D. 2020. Impact of small-scale tree planting patterns on outdoor cooling and thermal comfort. *Sustainable Cities and Society*. 56: 102085. https://doi.org/10.1016/j.scs.2020.102085

Ackerman, B. 1985. Temporal march of the Chicago heat island. *Journal of Climate and Applied Meteorology*. 24: 547-554. https://doi.org/10.1175/1520-0450(1985)024%3C0547:TMOTCH%3E2.0.CO;2

Albertsson Wikland, K., Luo, Z.C., Niklasson, A. and Karlberg, J. 2002. Swedish population-based longitudinal reference values from birth to 18 years of age for height, weight and head circumference. Acta Paediatr. 91(7): 739-754. https://doi.org/10.1080/08035250213216

ASHRAE. 2001. Fundamentals Handbook 2001 SI Edition. American Society of Heating, Refrigerating and Air Conditioning Engineers. ISBN 1883413885.

Awanou, C.N. 1998. Clear sky emissivity as a function of the zenith direction. *Renewable Energy*. 13(2): 227-248. https://doi.org/10.1016/S0960-1481(97)00070-0

Beck, H., Zimmermann, N. and McVicar, T. 2018. Present and future Köppen-Geiger climate classification maps at 1-km resolution. Sci. Data. 5: 180214. https://doi.org/10.1038/sdata.2018.214

Bernard, J., Lindberg, F. and Oswald, S. 2021. Urban wind field calculation through the Röckle based method: the basics for a GIS implementation. EMS Annual Meeting Abstracts. 18: EMS2021-27. https://doi.org/10.5194/ems2021-27

Blazejczyk, K., Broede, P., Fiala, D., Havenith, G., Holmér, I., Jendritzky, G., Kampmann, B. and Kunert, A. 2010. Principles of the new universal thermal comfort index (UTCI) and its application to bioclimatic research in European scale. *Miscellanea Geographica*. 14(1): 91-102. https://doi.org/10.2478/mgrsd-2010-0009

Bliss, R.W. 1961. Atmospheric Radiation Near the Surface of the Ground: A Summary for Engineers. *Solar Energy*. 5(3): 103-120. https://doi.org/10.1016/0038-092X(61)90053-6

Brown, R.D. 2011. Ameliorating the effects of climate change: Modifying microclimates through design. *Landscape and Urban Planning*. 100(4): 372-374. https://doi.org/10.1016/j.landurbplan.2011.01.010

Brown, R.D. and Gillespie. T.J. 1986. Estimating outdoor thermal comfort using a cylindrical radiation thermometer and an energy budget model. *Int. J. Biometeorol.* 30(1): 43-52. https://doi.org/10.1007/BF02192058

Bruse, M. and Fleer, H. 1998. Simulating surface-plant air interactions inside urban environments with a three dimensional numerical model. *Environ. Model. Softw.* 13(3-4): 373-384. https://doi.org/10.1016/S1364-8152(98)00042-5

Buras, A., Rammig, A. and Zang, C.S. 2020. Quantifying impacts of the 2018 drought on European ecosystems in comparison to 2003. *Biogeosciences*. 17: 1655-1672. https://doi.org/10.5194/bg-17-1655-2020

Butte, N.F., Watson, K.B., Ridley, K., Zakeri, I.F., McMurray, R.G., Pfeiffer, K.A., Crouter, S.E., Herrmann, S.D., Bassett, D.R., Long, A., Berhane, Z., Trost, S.G., Ainsworth, B.E., Berrigan, D. and Fulton, J.E. 2018. A youth compendium of physical activities. Activity codes and metabolic intensities. Medicine & Science in Sports & Exercise. 50 (2): 246-256. https://doi.org/10.1249/mss.0000000000001430

Chen, H., Ooka, R. and Kato, S. 2008. Study on optimum design method for pleasant outdoor thermal environment using genetic algorithms (GA) and coupled simulation of convection, radiation and conduction. *Building and Environment.* 43: 18-30. https://doi.org/10.1016/j.buildenv.2006.11.039

Cheng, W. 2020. Design of thermally comfortable and uvr-healthy schoolyards for children in low latitude urban areas in North America (College Station, TX). Doctoral Thesis. Texas A&M University, Texas, USA. https://hdl.handle.net/1969.1/192223

Cheng, W. and Brown. R.D. 2020. An energy budget model for estimating the thermal comfort of children. *Int. J. Biometeorol*. 64: 1355-1366. https://link.springer.com/article/10.1007/s00484-020-01916-x

Collins, W.J., Bellouin, N., Doutriaux-Boucher, M., Gedney, N., Halloran, P., Hinton, T., Hughes, J., Jones, C.D., Joshi, M., Liddicoat, S., Martin, G., O'Connor, F., Rae, J., Senior, C., Sitch, S., Totterdell, I., Wiltshire, A. and Woodward, S. 2011. Development and evaluation of an Earth-System model – HadGEM2. *Geosci. Model Dev*. 4: 1051-1075. https://doi.org/10.5194/gmd-4-1051-2011

Christensen, O.B., Kjellström, E., Dieterich, C., Gröger, M. and Meier, H.E.M. 2022. Atmospheric regional climate projections for the Baltic Sea region until 2100. *Earth Syst. Dynam*. 13: 133-157. https://doi.org/10.5194/esd-13-133-2022

Dines, W.H. and Dines, L.H.G. 1927. Monthly means of radiation from various parts of the sky at Benson, Oxfordshire. Mem. R. Met. Soc. 2 (11). https://doi.org/10.1002/qj.49705523108.

Dufresne, J-L., Foujols, M-A., Denvil, S., Caubel, A., Martin, O., Aumont, O., Balkanski, Y., Bekki, S., Bellenger, H., Benshila, R., Bony, S., Bopp, L., Braconnot, P., Brockmann, P., Cadule, P., Cheruy, F., Codron, F., Cozic, A., Cugnet, D., de Noblet, N., Duvel, J-P., Ethé, C., Fairhead, L., Fichefet, T., Flavoni, S., Friedlingstein, P., Grandpeix, J-Y., Guez, L., Guilyardi, E., Hauglustaine, D., Hourdin, F., Idelkadi, A., Ghattas, J., Joussaume, S., Kageyama, M., Krinner, G., Labetoulle, S., Lahellec,

A., Lefebvre, M-P., Lefevre, F., Levy, C., Li, Z.X., Lloyd, J., Lott, F., Madec, G., Mancip, M., Marchand, M., Masson, S., Meurdesoif, Y., Mignot, J., Musat, I., Parouty, S., Polcher, J., Rio, C., Schulz, M., Swingedouw, D., Szopa, S., Talandier, C., Terray, P., Viovy, N. and Vuichard, N. 2013. Climate change projections using the IPSL-CM5 Earth System Model: from CMIP3 to CMIP5. *Climate Dynamics*. 40: 2123-2165. https://doi.org/10.1007/s00382-012-1636-1

Elasser, W.M. 1942. Heat transfer by radiation in the atmosphere. Harv. Met. Stud. No. 6. Harvard University Press, Cambridge, Massachusetts.

Eliasson, I. 1996. Intra-urban nocturnal temperature differences: a multivariate approach. *Climate research*. 7: 21-30. https://doi.org/10.3354/cr007021

Erell, E. and Williamson, T. 2007. Intra-urban differences in canopy layer air temperature at a mid-latitude city. *Int. J. Climatol*. 27: 1243-1255. https://doi.org/10.1002/joc.1469

Erell, E., Pearlmutter, D., Boneh, D. and Kutiel, P.B. 2014. Effect of high-albedo materials on pedestrian heat stress in urban street canyons. *Urban Climate*. 10: 367-386. https://doi.org/10.1016/j.uclim.2013.10.005

Falk, B. and Dotan, R. 2008. Children's thermoregulation during exercise in the heat: a revisit. *Appl. Physiol. Nutr. Metab*. 33(2): 420-7. https://doi.org/10.1139/h07-185

Fallman, J., Emeis, S. and Suppan, P., 2013. Mitigation of urban heat stress – a modelling case study for the area of Stuttgart. *Die Erde – Journal of the Geographical Society of Berlin*. 144(3-4): 202-16. https://doi.org/10.12854/erde-144-15

Fanger, P.O. 1970. Thermal Comfort: Analyses and Applications in Environmental Engineering. McGraw Hill, New York. 244p.

Fiala, D., Havenith, G., Bröde, P., Kampmann, B. and Jendritzky, G. 2012. UTCI-Fiala multi-node model of human heat transfer and temperature regulation. *Int. J. Biometeorol*. 56(3): 429-441. https://doi.org/10.1007/s00484-011-0424-7

Folkhälsomyndigheten. 2015. Hälsoeffekter av höga temperaturer – En kunskapssammanställning. Folkhälsomyndigheten, artikelnummer: 15048. ISBN 978-91-7603-487-3

Folkhälsomyndigheten. 2017. Att hantera hälsoeffekter av värmeböljor – Vägledning till handlingsplaner. Folkhälsomyndigheten, artikelnummer: 21154.

Folkhälsomyndigheten. 2018. Värmestress I urbana utomhusmiljöer – Förekomst och åtgärder i befintlig bebyggelse. Folkhälsomyndigheten, artikelnummer: 18061.

Folkhälsomyndigheten. 2021. Riktlinjer för fysisk aktivitet och stillasittande – Kunskapsstöd för främjande av fysisk aktivitet och minskat stillasittande. Folkhälsomyndigheten, artikelnummer: 21099.

Gabriel, K.M.A. and Endlicher, W.R. 2011. Urban and rural mortality rates during heat waves in Berlin and Brandenburg, Germany. *Environ. Pollut*. 159: 2044–2050. https://doi.org/10.1016/j.envpol.2011.01.016

Gal, C.V. and Kántor, N. 2020. Modeling mean radiant temperature in outdoor spaces, A comparative numerical simulation and validation study. *Urban Climate*. 32: 100571. https://doi.org/10.1016/j.uclim.2019.100571

Giorgetta A., M.A., Jungclaus, J., Reick, C.H., Legutke, S., Bader, J., Böttinger, M., Brovkin, V., Creuger, T., Esch, M., Fieg, K., Glushak, K., Gayler, V., Haak, H., Hollweg, H-D., Ilyina, T., Kinne, S., Kornblueh, L., Matei, D., Mauritsen, T., Mikolajewicz, U., Mueller, W., Notz, D., Pithan, F., Raddatz, T., Rast, S., Redler, R., Roeckner, E., Schmidt, H., Schnur, R., Segschneider, J., Six, K.D., Stockhause, M., Timmreck, C., Wegner, J., Widmann, H., Wieners, K-H., Claussen, M., Marotzke, J. and Stevens, B. 2013. Climate and carbon cycle changes from 1850 to 2100 in MPI-ESM simulations for the Coupled Model Intercomparison Project phase 5. *Journal of Advances in Modeling Earth Systems*. 5(3): 572-597. https://doi.org/10.1002/jame.20038

Hazeleger, W., Wang, X., Severijns, C., Stefanscu, S., Bintanja, R., Sterl, A., Wyser, K., Semmler, T., Yang, S., van den Hurk, B., van Noije, T., van der Linden, E. and van der Wiel, K. 2011. EC-Earth V2.2: description and validation of a new seamless earth system prediction model. *Climate Dynamics*. 39: 2611-2629. https://doi.org/10.1007/s00382-011-1228-5

Holmer, B., Thorsson, S. and Eliasson, I. 2007. Cooling rates, sky view factors and the development of intra-urban air temperature differences. *Geogr. Ann*. 89A(4): 237-248. https://doi.org/10.1111/j.1468-0459.2007.00323.x

Holmer, B., Thorsson, S. and Lindén, J. 2013. Evening evapotranspirative cooling in relation to vegetation and urban geometry in the city of Ouagadougou, Burkina Faso. *Int. J. Climatol*. 33(15): 3089-105. https://doi.org/10.1002/joc.3561

Holmer, B., Lindberg, F., Rayner, D. and Thorsson, S. 2015. How to transform the standing man from a box to a cylinder – a modified methodology to calculate mean radiant temperature in field studies and models. ICUC9 – 9th International Conference on Urban Climate jointly with 12th Symposium on the Urban Environment. BPH5: Human perception and new indicators. Toulouse, July 2015.

Howard, L. 1833. The climate of London deduced from meteorological observations made in the metropolis and at various places around it. London, Harvey and Darton, J. and A. Arch, Longman, Hatchard, S. Highly and R. Hunter.

Höppe, P. 1984. Die Energiebilanz des Menschen. Doctoral Thesis. Wiss Mitt Meteorol. Inst. Univ. München. 49.

Höppe, P. 1992. A new procedure to determine the mean radiant temperature outdoors. *Wetter und leben*. 44: 147-151.

Höppe, P. 1994. Die Wärmebilanzmodelle MEMI und IMEM zur Bewertung der thermischen Beanspruchung am Arbeitsplatz. *Verh Dtsch Ges Arbeitsmed Umweltmed*. 34: 153-158.

Höppe, P. 1999. The physiological equivalent temperature – a universal index for the biometeorological assessment of the thermal environment. *Int. J. Biometeorol*. 43: 71-75. https://doi.org/10.1007/s004840050118

Jonsson, P., Eliasson, I., Holmer, B. and Grimmond, C.S.B. 2006. Longwave incoming radiation in the Tropics: results from field work in three African cities. *Theor. Appl. Climatol*. 85: 185-201. http://dx.doi.org/10.1007/s00704-005-0178-4

Kántor, N., Lin, T-P. and Matzarakis, A. 2014. Daytime relapse of mean radiant temperature based on the six-directional method under unobstructed solar radiation. *Int. J. Biometeorol*. 58: 1615-1625. https://doi.org/10.1007/s00484-013-0765-5

Kántor, N., Gal, C.V., Gulyas, A. and Unger, J. 2018. The Impact of Façade Orientation and Woody Vegetation on Summertime Heat Stress Patterns in a Central European Square: Comparison of Radiation Measurements and Simulations. *Advances in Meteorology*. 2018: 2650642. https://doi.org/10.1155/2018/2650642

Kenny, N.A., Warland, J.S., Brown, R.D. and Gillespie, T.J. 2009a. Part A: Assessing the performance of the COMFA outdoor thermal comfort model on subjects performing physical activity. *Int. J. Biometeorol*. 53: 415-428. https://doi.org/10.1007/s00484-009-0226-3

Kenny, N.A., Warland, J.S., Brown, R.D. and Gillespie, T.J. 2009b. Part B: Revisions of the COMFA outdoor thermal comfort model for application to subjects performing physical activity. *Int. J. Biometeorol*. 53: 429-441. https://doi.org/10.1007/s00484-009-0227-2

Kipp & Zonen. 2009. CNR1 Net radiometer Instruction sheet. Delft, The Netherlands. Kipp & Zonen B.V. https://www.kippzonen.com/Download/86/Instruction-Sheet-Net-Radiometers-CNR1 last retrieved 2022-04-20.

Klimatanpassningsrådet. 2022. Första rapporten från Nationella expertrådet för klimatanpassning. Nationella Expertrådet För Klimatanpassning. Retrieved from https://klimatanpassningsradet.se/polopoly_fs/1.180289!/Rapport%20fr%C3%A5n%20Nationella%20expertr%C3%A5det%20f%C3%B6r%20klimatanpassning%202022.pdf last access 2022-04-19

Konarska, J., Lindberg, F., Larsson, A., Thorsson, S. and Holmer, B. 2014. Transmissivity of solar radiation through crowns of single urban trees – application for outdoor thermal comfort modelling. *Theor. Appl. Climatol*. 117: 363-376. https://doi.org/10.1007/s00704-013-1000-3

Kotlarski, S., Keuler, K., Christensen, O.B., Colette, A., Déque, M., Gobiet, A., Goergen, K., Jacob, D., Lüthi, D., van Meijergaard, E., Nikulin, G., Schär, C., Teichmann, C., Vautard, R., Warrach-Sagi, K. and Wulfmeyer, V. 2014. Regional climate modeling on European scales: a joint standard evaluation of the EURO-CORDEX RCM ensemble. *Geosci. Model Dev*. 7: 1297-1333. https://doi.org/10.5194/gmd-7-1297-2014

Kovats, R.S. and Hajat, S. 2008. Heat Stress and Public Health: A Critical Review. *Annu. Rev. Public Health.* 29: 41-55. https://doi.org/10.1146/annurev.publhealth.29.020907.090843

Krikken, F., Lehner, F., Haustein, K., Drobyshev, I. and van Oldenborgh, G.J. 2021. Attribution of the role of climate change in the forest fires in Sweden 2018. *Nat. Hazards Earth Syst. Sci*. 21: 2169-2179. https://doi.org/10.5194/nhess-21-2169-2021

Lee, H., Holst, J. and Mayer, H. 2013. Modification of human-biometeorologically significant radiant flux densities by shading as local method to mitigate heat stress in summer within urban street canyons. *Advances in Meteorol*. 2013: 312572. https://doi.org/10.1155/2013/312572

Lee, H., Mayer, H. and Kuttler, W. 2020. Impact of spacing between tree crowns on the mitigation of daytime heat stress for pedestrians inside E-W urban street canyons under Central European conditions. *Urban Forestry & Urban Greening*. 48: 126558. https://doi.org/10.1016/j.ufug.2019.126558

Lindberg, F., Holmer, B. and Thorsson, S. 2008. SOLWEIG 1.0 – modelling spatial variations of 3D radiant fluxes and mean radiant temperature in complex urban settings. *Int. J. Biometeorol.* 52: 697-713. https://doi.org/10.1007/s00484-008-0162-7

Lindberg, F. and Grimmond, S. 2011. The influence of vegetation and building morphology on shadow patterns and mean radiant temperatures in urban areas: model development and evaluation. *Theor. Appl. Climatol*. 105: 311-323. https://doi.org/10.1007/s00704-010-0382-8

Lindberg, F., Holmer, B., Thorsson, S. and Rayner, D. 2014. Characteristics of the mean radiant temperature in high latitude cities – implications for sensitive climate planning applications. *Int. J. Biometeorol*. 58: 613-627. https://doi.org/10.1007/s00484-013-0638-y

Lindberg, F., Thorsson, S., Rayner, D. and Lau, K. 2016. The impact of urban planning strategies on heat stress in a climate-change perspective. *Sustainable Cities and Society*. 25: 1-12. https://doi.org/10.1016/j.scs.2016.04.004

Lindberg, F., Grimmond, C.S.B., Gabey, A., Huang, B., Kent, C.W., Sun, T., Theeuwes, N.E., Järvi, L., Ward, H.C., Capel-Timms, I., Chang, Y., Jonsson, P., Krave, N., Liu, D., Meyer, D., Olofson, K.F.G., Tan, J., Wästberg, D., Xue, L. and Zhang, Z. 2018. Urban Multi-Scale Environmental Predictor (UMEP): An integrated tool for city-based climate services. *Environmental Modelling and Software*. 99: 70-87. https://doi.org/10.1016/j.envsoft.2017.09.020

Li, X. and Wang, G. 2021. GPU parallel computing for mapping urban outdoor heat exposure. *Theor. Appl. Climatol*. 145: 1101-1111. https://doi.org/10.1007/s00704-021-03692-z

Liu, Z. and Jim, C.Y. 2021. Playing on natural or artificial turf sports fields? Assessing heat stress of children, young athletes and adults in Hong Kong. *Sustainable Cities and Society*. 75: 103271. https://doi.org/10.1016/j.scs.2021.103271

Luke, S., 2013. Essentials of Metaheuristics, Lulu, second edition, available for free at http://cs.gmu.edu/~sean/book/metaheuristics/

Malmquist, A., Lundgren, T., Hjerpe, M., Glaas, E., Turner, E. and Storbjörk, S. 2021. Vulnerability and adaptation to heat waves in preschools: Experiences, impacts and responses by unit heads, educators and parents. *Climate Risk Assessment*. 31: 100271. https://doi.org/10.1016/j.crm.2020.100271

Maronga, B., Gryschka, M., Heinze, R., Hoffmann, F., Kanani-Sühring, F., Keck, M., Ketelsen, K., Letzel, M.O., Sühring, M. and Raasch, S. 2015. The parallelized large-eddy simulation model (PALM) version 4.0 for atmospheric and oceanic flows: Model formulation, recent developments, and future perspectives. *Geoscientific model development*. 8(8): 2515-2551. https://doi.org/10.5194/gmd-8-2515-2015

Martin, M. and Berdahl, P. 1984. Summary of results for the spectral and angular sky radiation measurement program. *Solar Energy*. 33(3-4): 241-252. https://doi.org/10.1016/0038-092X(84)90155-5

Matzarakis, A., Mayer, H. and Iziomon, M.G. 1999. Applications of a universal thermal index: physiological equivalent temperature. *Int. J. Biometeorol*. 43: 76-84. https://doi.org/10.1007/s004840050119

Matzarakis, A., Rutz, F. and Mayer, H. 2007. Modelling radiation fluxes in simple and complex environments – application of the RayMan model. *Int. J. Biometeorol.* 51 (4): 323-334. https://doi.org/10.1007/s00484-006-0061-8

Matzarakis, A., Rutz, F. and Mayer, H. 2010. Modelling radiation fluxes in simple and complex environments: basics of the RayMan model. *Int. J. Biometeorol*. 54: 131-139. https://doi.org/10.1007/s00484-009-0261-0

Mayer, H. and Höppe, P. 1987. Thermal Comfort of Man in Different Urban Environments. *Theor. Appl. Climatol*. 38: 43-49. https://doi.org/10.1007/BF00866252

Mayer, H., Holst, J., Dostal, P., Imbery, F. and Schindler, D. 2008. Human thermal comfort in summer within an urban street canyon in Central Europe. *Meteorologische Zeitschrift*. 17(3): 241-250. https://doi.org/10.1127/0941-2948/2008/0285

McArthur, L.J.B. and Hay, J.E. 1981. A Technique for Mapping the Distribution of Diffuse Solar Radiation over the Sky Hemisphere. *J. Appl. Meteorol*. 20(4): 421-429. https://doi.org/10.1175/1520-0450(1981)020%3C0421:ATFMTD%3E2.0.CO;2

Moss, R.H., Edmonds, J.A., Hibbard, K.A., Manning, M.R., Rose, S.K., van Vuuren, D.P., Carter, T.R., Emori, S., Kainuma, M., Kram, T., Meehl, G.A., Mitchell, J.F.B., Nakicenovic, N., Riahi, K., Smith, S.J., Stouffer, R.J., Thomson, A.M., Weyant, J.P. and Wilbanks, T.J. 2012. The next generation of scenarios for climate change research and assessment. *Nature*. 463: 747-756. https://doi.org/10.1038/nature08823

Musy, M., Malys, L., Morille, B. and Inard, C. 2015. The use of SOLENE-microclimat model to assess adaptation strategies and the district scale. *Urban Climate.* 14 (part 2): 213-223. https://doi.org/10.1016/j.uclim.2015.07.004

Mårtensson, F. 2004. Landskapet i leken – En studie av utomhuslek på förskolegården. Doctoral thesis, Acta Universitatis agriculturae Sueciae. Agraria, 464. ISBN 91-576-6489-7. Swedish University of Agricultural Sciences, Alnarp, Sweden. https://pub.epsilon.slu.se/803/

Nahon, R., Paz Acuña y Miño, J. and Beckers, B. 2019. Exploring the Sky Longwave Radiance Distribution in the French Basque Country. Proceedings of the 16th IBPSA Conference, Rome, Italy, Sept. 2-4, 2019. 4134-4140. https://doi.org/10.26868/25222708.2019.210351

Nikolopoulou, M., Baker, N. and Steemers, K. 1999. Improvements of the globe thermometer for outdoor use. *Architectural Science Review*. 42 (1): 27-34.

Nikulin, G., Kjellström, E., Hansson, U., Strandberg, G. and Ullerstig, A. 2011. Evaluation and future projections of temperature, precipitation and wind extremes over Europe in an ensemble of regional climate simulations. *Tellus A: Dynamic Meteorology and Oceanography*. 63(1): 41-55. https://doi.org/10.1111/j.1600-0870.2010.00466.x

Oke, T.R. 1973. City size and the urban heat island. *Atmospheric Environment*. 7 (8): 769-779. https://doi.org/10.1016/0004-6981(73)90140-6

Oke, T.R. 1981. Canyon geometry and the nocturnal urban heat island: comparison of scale model and field observations. *Journal of Climatology*. 1: 237-254. https://doi.org/10.1002/joc.3370010304

Oke, T.R. 1982. The energetic basis of the urban heat island. *Quart. J. R. Met. Soc*. 108: 1-24. https://doi.org/10.1002/qj.49710845502

Oke, T.R. 1988. The urban energy balance. Progress in Physical Geography: *Earth and Environment*. 12 (4): 471-508. https://doi.org/10.1177%2F030913338801200401

Oke, T.R., Mills, G., Christen, A. and Voogt, J.A. 2017. Urban Climates. Cambridge University Press. https://doi-org.ezproxy.ub.gu.se/10.1017/9781139016476

Ooka, R., Chen, H. and Kato, S. 2008. Study on optimum arrangement of trees for design of pleasant outdoor environment using multi-objective genetic algorithm and coupled simulation of convection, radiation and conduction. *Journal of Wind Engineering and Industrial Aerodynamics*. 96, 1733-1748. https://doi.org/10.1016/j.jweia.2008.02.039

Oudin Åström, D., Forsberg, B., Ebi, K.L and Rocklöv, J. 2013. Attributing mortality from extreme temperatures to climate change in Stockholm, Sweden. *Nature Climate Change*. 3: 1050-1054. https://doi.org/10.1038/nclimate2022

Perez, R., Seals, R. and Michalsky, J. 1993. All-weather model for sky illuminance distribution – preliminary configuration and validation. *Sol. Energy*. 50 (3): 235-246. https://doi.org/10.1016/0038-092X(93)90017-I

Prata, A.J. 1996. A new long-wave formula for estimating downward clear-sky radiation at the surface. *Q. J. Meteorol. Soc*. 122: 1127-1151. https://doi.org/10.1002/qj.49712253306

Rayner, D., Lindberg, F., Thorsson, S. and Holmer, B. 2014. A statistical downscaling algorithm for thermal comfort applications. *Theor. Appl. Climatol*., 122: 729-742. https://doi.org/10.1007/s00704-014-1329-2

Rayner, D., Lindberg, F., Kukulies, J., Thorsson, S. and Wallenberg, N. 2021. Urban climate data for Gothenburg, 1983-2020. University of Gothenburg, Department of Earth Sciences. Swedish National Data Service. Version 1. https://doi.org/10.5878/a2h2-4s63

Reindl, D.T., Beckman, W.A. and Duffie, J.A. 1990. Diffuse fraction correlations. *Solar Energy*. 45(1): 1-7. https://doi.org/10.1016/0038-092X(90)90060-P

Robinson, G.D. 1947. Notes on the measurement and estimation of atmospheric radiation. *Quart. J. R. Met. Soc*. 73: 127-150. https://doi.org/10.1002/qj.49707331510

Robinson, G.D. 1950. Notes on the measurement and estimation of atmospheric radiation. *Quart. J. R. Met. Soc*. 76: 37-51. https://doi.org/10.1002/qj.49707632705

Robinson, D. and Stone, A. 2004. Solar radiation modelling in the urban context. *Sol. Energy*. 77: 295-309. https://doi.org/10.1016/j.solener.2004.05.010

Robinson, D. and Stone, A. 2005. A simplified radiosity algorithm for general urban radiation exchange. *Build. Serv. Eng. Res. Technol*. 26 (4): 271-284. https://doi.org/10.1191%2F0143624405bt133oa

Rocklöv, J. and Forsberg, B. 2008. The effect of temperature on mortality in Stockholm 1998-2003: a study of lag structures and heatwave effects. *Scand. J. Public Health*. 36(5): 516-523. https://doi.org/10.1177/1403494807088458

Rocklöv, J., Ebi, K. and Forsberg, B. 2011. Mortality related to temperature and persistent extreme temperatures: a study of cause-specific and age-stratified mortality. *Occupational and Environmental Medicine.* 68: 531-536. http://dx.doi.org/10.1136/oem.2010.058818

Samuelsson, P., Jones, C.G., Willén, U., Ullerstig, A., Gollvik, S., Hansson, U., Jansson, C., Kjellström, E., Nikulin, G. and Wyser, K. 2011. The Rossby Centre regional climate model RCA3: model description and performance. *Tellus A: Dynamic Meteorology and Oceanography*. 63(1): 4-23. https://doi.org/10.1111/j.1600-0870.2010.00478.x

SCB. 2022a. Tätorter i Sverige. Retrieved from https://www.scb.se/hitta-statistik/sverige-i-siffror/miljo/tatorter-i-sverige/ last access: 2022-04-19.

SCB. 2022b. Folkmängd, topp 50 – 31 december 2021. Statistikmyndigheten. Last update 2022-02-22. https://www.scb.se/hitta-statistik/statistik-efter-amne/befolkning/befolkningens-sammansattning/befolkningsstatistik/pong/tabell-och-diagram/topplistor-kommuner/folkmangd-topp-50/ Last access: 2022-03-15.

Schofield, W.N. 1985. Predicting basal metabolic rate, new standards and review of previous work. *Human nutrition. Clin Nutr.* 39: 5-41.

Shannon, H., Stewart, I. and Stewart, K. 2009. Preventing physical activity induced heat illness in school settings. Proceedings of the 26th ACHPER Int. Conference: Creating active futures. School of human movement studies, Queensland University of Technology. 271-281.

Simon, H. 2016. Modeling urban microclimate. Development, implementation and evaluation of new and improved calculation methods for the urban microclimate model ENVI-met. Doctoral thesis. Johannes Gutenberg-Universität Mainz. http://doi.org/10.25358/openscience-4042

Sjöman, J.D., Hirons, A. and Sjöma, H. 2015. Branch Area Index of Solitary Trees: Understanding Its Significance in Regulating Ecosystem Services. *J. Environ. Qual.* 45: 175-187. https://doi.org/10.2134/jeq2015.02.0069

Srivanit, M. and Jareemit, D. 2020. Modeling the influences of layouts of residential townhouses and tree-planting patterns on outdoor thermal comfort in Bangkok suburb. *Journal of Building Engineering*. 30: 101262.

Stojakovic, V., Bajsanski, I., Savic, S., Milosevic, D. and Tepavcevic, B. 2020. The influence of changing location of trees in urban green spaces on insolation mitigation. *Urban Forestry & Urban Greening*. 126721. https://doi.org/10.1016/j.ufug.2020.126721

Sundborg, Å. 1950. Local climatological studies of the temperature conditions in an urban area. *Tellus 2*: 221-231.

Sundborg, Å. 1951. Climatological studies in Uppsala with special regard to the temperature conditions in the urban area. *Geographica 22*.

Taylor, K.E., Stouffer, R.J. and Meehl, G.A. 2012. An overview of CMIP5 and the experiment design. *Bulletin of the American Meteorological Society*. 93(4): 485-498. https://doi.org/10.1175/BAMS-D-11-00094.1

Thorsson, S., Lindberg, F., Eliasson, I. and Holmer, B. 2007. Different methods for estimating mean radiant temperature in an outdoor urban setting. *Int. J. Climatol*. 27: 1983-1993. https://doi.org/10.1002/joc.1537

Thorsson, S., Lindberg, F., Björklund, J., Holmer, B. and Rayner, D. 2011. Potential changes in outdoor thermal comfort conditions in Gothenburg, Sweden due to climate change: the influence of urban geometry. *Int. J. Climatol*. 31: 324-335. https://doi.org/10.1002/joc.2231

Thorsson, S., Rocklöv, J., Konarska, J., Lindberg, F., Holmer, B., Dousset, B. and Rayner, D. 2014. Mean radiant temperature – A predictor of heat related mortality. *Urban Climate.* 10: 332-345. https://doi.org/10.1016/j.uclim.2014.01.004

Thorsson, S., Rayner, D., Lindberg, F., Monteiro, A., Katzschner, L., Lau, K.K-L., Campe, S., Katzschner, A., Konarska, J., Onomura, S., Velho, S. and Holmer, B. 2017. Present and projected future mean radiant temperature for three European cities. *Int. J. Biometeorol*. 61: 1531-1543. https://doi.org/10.1007/s00484-017-1332-2

Tjiputra, J.F., Roelandt, C., Bentsen, M., Lawrence, D.M., Lorentzen, T., Schwinger, J., Seland, Ö. and Heinze, C. 2013. Evaluation of the carbon cycle components in the Norwegian Earth System Model (NorESM). *Geosci. Model Dev*. 6: 301-325. https://doi.org/10.5194/gmd-6-301-2013

Tregenza, P. 1987. Subdivision of the sky hemisphere for luminance measurements. *Light. Res. Technol*. 19 (1): 13-14. https://doi.org/10.1177%2F096032718701900103

UN, 2015. Transforming our World: The 2030 Agenda for Sustainable Development. A/RES/70/1. Retrieved from https://sustainabledevelopment.un.org/content/documents/21252030%20Agenda%20for%20Sustainable%20Development%20web.pdf 2022-04-15.

UN, 2018. 68% of the world population projected to live in urban areas by 2050, says UN. Retrieved from https://www.un.org/development/desa/en/news/population/2018-revision-of-world-urbanization-prospects.html 2020-09-11

Unsworth, M.H. and Monteith, J.L. 1975. Long-wave radiation at the ground I. Angular distribution of incoming radiation. *Quart. J. R. Met. Soc*. 101: 13-24. https://doi.org/10.1002/qj.49710142703

Vanos, J.K., Warland, J.S., Gillespie, T.J. and Kenny, N.A. 2012a. Thermal comfort modelling of body temperature and physiological variations of a human exercising in an outdoor environment. *Int. J. Biometeorol*. 56: 21-32. https://doi.org/10.1007/s00484-010-0393-2

Vanos, J.K., Warland, J.S., Gillespie, T.J. and Kenny, N.A. 2012b. Improved predictive ability of climate-human-behavior interactions with modifications to the COMFA outdoor energy budget model. *Int. J. Biometeorol*. 56: 1065-1074. https://doi.org/10.1007/s00484-012-0522-1

Vanos, J.K., Warland, J.S., Gillespie, T.J., Slater, G.A., Brown, R.D. and Kenny, N. 2012c. Human energy budget modeling in urban parks in Toronto and applications to emergency heat stress preparedness. *Journal of Applied Meteorology and Climatology*. 51 (9): 1639-1653. https://doi.org/10.1175/JAMC-D-11-0245.1

Vanos, J.K., Middel, A., McKercher, G.R., Kuras, E.R. and Ruddell, B.L. 2016. Hot playgrounds and children's health: A multiscale analysis of surface temperatures in Arizona, USA. *Landscape and Urban Planning*. 146: 29-42. https://doi.org/10.1016/j.landurbplan.2015.10.007

Vanos, J.K., Herdt, A.J. and Lochbaum, M.R. 2017. Effects of physical activity and shade on the heat balance and thermal perceptions of children in a playground microclimate. *Building and Environment*. 126: 119-131. https://doi.org/10.1016/j.buildenv.2017.09.026

Vautard, R., Gobiet, A., Jacob, D., Belda, M., Colette, A., Deque, M., Fernandez, J., Garcia-Diez, M., Goergen, K., Güttler, I., Halenka, T., Karacostas, T., Katragkou, E., Keuler, K., Kotlarski, S., Mayer, S., van Meijergaard, E., Nikulin, G., Patarcic, M., Scinocca, J., Sobolowski, S., Suklitsch, M., Teichmann, C., Warrach-Sagi, K., Wulfmeyer, V. and Yiou, P. 2013. The simulation of European heat waves from an ensemble of regional climate models within the EURO-CORDEX project. *Clim. Dyn*. 41: 2555-2575. https://doi.org/10.1007/s00382-013-1714-z

Voldoire, A., Sanchez-Gomez, E., Salas y Melia, D., Decharme, B., Cassou, C., Senesi, S., Valcke, S., Beau. I., Alias, A., Chevallier, M., Deque, M., Deshayes, J., Douville, H., Fernandez, E., Madec, G., Maisonnave, E., Moine, M-P., Planton, S., Saint-Martin, D., Szopa, S., Tyteca, S., Alkama, R., Belamari, S., Braun, A., Coquart, L. and Chauvin, F. 2012. The CNRM-CM5.1 global climate model: description and basic

evaluation. *Climate Dynamics*. 40: 2091-2121. https://doi.org/10.1007/s00382-011-1259-y

Wilcke, R.A.I., Kjellström, E., Lin, C., Matei, D., Moberg, A. and Tyrlis, E. 2020. The extremely warm summer of 2018 in Sweden – set in a historical context. *Earth Syst. Dynam*. 11: 1107-1121. https://doi.org/10.5194/esd-11-1107-2020

Wood, J. 2019. User manual for the Sunshine Pyranometer type SPN1. User Manual Version: 4.2, (ed) Nick Webb. Peak Design Ltd, Winster, Derbyshire, UK. Delta-T Devices Limited. https://delta-t.co.uk/wp-content/uploads/2019/06/SPN1_User_Manual_4.2.pdf last access 2021-11-09

Zhou, B., Rybski, D. and Kropp, J.P. 2017. The role of city size and urban form in the surface urban heat island. *Scientific Reports.* 7: 4791. https://doi.org/10.1038/s41598-017-04242-2

Zhao, Q., Wentz, E.A. and Murray, A.T. 2017. Tree shade coverage optimization in an urban residential environment. *Building and Environment*. 115, 269-280. https://doi.org/10.1016/j.buildenv.2017.01.036

Zhao, Q., Sailor, D.J. and Wentz, E.A. 2018. Impact of tree locations and arrangements on outdoor microclimates and human thermal comfort in an urban residential environment. *Urban Forestry & Urban Greening*. 32: 81-91. https://doi.org/10.1016/j.ufug.2018.03.022

Åström, C., Bjelkmar, P. and Forsberg, B. 2019. Attributing summer mortality to heat during 2018 heatwave in Sweden. *Environ. Epidemiol*. 3: 16-17. https://doi.org/10.1097/01.EE9.0000605788.56297.b5